DRAL
Daresbury Laboratory
Rutherford Appleton Laboratory

RAL Report
RAL-95-018

Ground-Based Measurements in Support of CLUSTER: An On-Line Planning Procedure

Lockwood et al

February 1995

Rutherford Appleton Laboratory Chilton DIDCOT Oxfordshire OX11 0QX

Ground-Based Measurements in Support of CLUSTER: An On-Line Planning Procedure

M. Lockwood, R. Stamper and M.N. Wild

(World Data Centre C1 for Solar Terrestrial Physics, Rutherford Appleton Laboratory, Chilton, Didcot, OX11 0QX, UK)

and H.J. Opgenoorth

(IRF, Swedish Institute for Space Physics, Uppsala Division, S-75591 Uppsala, Sweden)

RAL Report
RAL-95-018

RAL

Cluster/Ground-based Data Centre WDC-C1

Abstract

The four Cluster spacecraft offer a unique opportunity to study structure and dynamics of the magnetosphere and we discuss four general ways in which ground-based remote-sensing observations of the ionosphere can be used to support the in-situ measurements. There are a very large number of potentially useful configurations between the satellites and any one ground-based observatory; however, the number of ideal occurrences for any one configuration is low. Many of the ground-based instruments cannot operate continuously and Cluster will take data for only 50% of each orbit, on average. In addition, there are a great many instrument modes and the orientation, size and shape of the cluster of the four satellites to consider. There is a clear and pressing need for careful planning to ensure that the scientific return from Cluster is maximised by the ground-based observations. For this reason, the European Space Agency (ESA) established a working group to coordinate the observations. We present an on-line procedure to plan coordinated measurements by the Cluster spacecraft with the combined ground-based systems. We illustrate the philosophy of the method, using two important examples of the many possible configurations between the satellite and the ground-based instruments. In section 5 we describe how experimenters using ground-based facilities can utilise this software, via World-Wide Web, and how the information collected will be used as input into ESA's planning for Cluster operations.

RAL Report
RAL-95-018
Rutherford Appleton Laboratory, Chilton, Didcot, OX11 0QX, UK

Contents

Parts of this report are from the paper "Opportunities for magnetospheric research using EISCAT/ESR and CLUSTER", by M. Lockwood and H.J. Opgenoorth, submitted to the special issue of *J. Geoelect. Geomag.*, on the Japan-EISCAT Symposium on the Polar Ionosphere (JESPI), held at Toba, Ise-Shima, Japan, August/September 1994.

1. Introduction

One of the most active areas of solar-terrestrial physics research in recent years has been the study of transient events and rapid temporal changes in the magnetosphere-ionosphere system. Ground-based remote-sensing observations have a vital role to play in these studies because they are unique in covering a range of invariant latitudes, at high time resolution and for an extended period of time. In-situ satellite observations, on the other hand, provide much higher resolution data but suffer from either spatial-temporal ambiguity (at low altitudes) or from limited spatial coverage (at high altitudes). For both remote sensing and in-situ measurements, there is a compromise struck between spatial coverage, time resolution and the length of the continuous data sequence in any one region of the coupled magnetosphere-ionosphere system. For in-situ observations this compromise is set by the orbital dynamics of the satellite; for spatially-integrating ground-based instruments (like magnetometers) it is set by the rotation period of the Earth; but for instruments like radars and imaging riometers, with multiple or steerable beams, this choice can be varied within broad limits set by the rotation of the Earth and the scanning capabilities of the instrument.

Not only are there problems of distinguishing spatial structure from temporal changes in data from a lone spacecraft, but also we cannot determine the motion nor the orientation of observed structures and boundaries. These problems will be addressed in three dimensions for the first time by the four Cluster spacecraft (*Schmidt and Goldstein*, 1988), flying in known but variable configurations (*Rodriguez-Canabal et al.*, 1993; *Balogh et al.*, 1993). However, they will only answer questions on certain temporal and spatial scales, depending on their separation vectors and altitude (and hence velocity). Ground-based observations can be used in a number of ways to provide important support for Cluster data and greatly enhance the mission's scientific return.

In terms of the number of geophysical parameters measured, the most powerful of the ground-based observatories are the incoherent scatter (IS) radars, which can be used to measure ion drifts (electric fields), ion and electron temperatures and plasma density. With models and complex processing, the radars also indirectly yield much more information, including conductivities, neutral winds and precipitating electron spectra. By the time Cluster data-taking commences in 1996, the EISCAT Svalbard Radar, ESR, (*Cowley et al.*, 1990) will be in operation on the island of Spitsbergen and this will add to the existing high-latitude IS facilities at Sondrestromfjord, Millstone Hill and EISCAT. The range and flexibility of these radars allows detailed measurements to be made which will be exciting complements to the Cluster observations. However, it will be important to match the operating modes to the satellite observations, such that the radars genuinely add to the information that the satellites obtain. For example, in order to achieve the right balance between spatial coverage and temporal resolution, the antenna scanning pattern appropriate to each study will be needed. Similarly, the right balance between spatial and temporal resolution will need to be struck by the antenna scanning pattern and the pulse coding scheme. A key point about IS radars is that they require much maintenance and cannot operate on a continuous basis. Therefore detailed planning is required to ensure that the best opportunities for combined studies with Cluster are exploited.

In addition, HF backscatter radars can provide vital 2-dimensional snapshots of the convective

flow (*Hanuise et al.*, 1993) and the SUPERDARN network currently under construction will image such flow patterns over a large fraction of the high-latitude region in the northern hemisphere. In addition, a tri-static system is planned in the Southern hemisphere, allowing conjugate studies. These systems can take data almost continuously; however, operations planning is still required as they can employ a variety of modes and it will be important that the scan patterns selected are the most appropriate to the combined observations. There are also a wide variety of ground-based optical instruments, which can reveal transient events and track evolving boundaries. Networks of magnetometers, imaging riometers, and digital ionosondes all have many other important applications including monitoring the latitude of the auroral oval as well as the extent and intensity of disturbances along it. Some of these ground-based instruments run continuously, whereas others are operated on a campaign basis. Campaigns will require careful planning if the scientific return with Cluster observations are to be maximised. In this report we do not wish to review the many capabilities of all these instruments. Rather we wish to present and explain a procedure which aims to ensure that they will be used to maximum effect during the Cluster mission.

From a survey of the literature we have defined four classes of scientific investigations, employing simultaneous satellite and ground-based observations. We do not attempt to review all such measurements here, but give selected examples to illustrate the classes of application and to look at their potential for combined Cluster and ground based observations.

(i) Resolution of spatial and temporal variations.

The ground-based data can extend the range of time scales of temporal variations which can be studied and can also be used to interpolate between data taken at different times by different Cluster craft at a given point in space. Recent examples of this kind of application (with lone satellites) have included studies of precipitation of magnetosheath-like plasma in what we now know to be transient events called travelling convection vortices (TCVs), as detected by conjugate arrays of ground-based magnetometers and radars (*Potemra et al.*, 1992; *Heikkila et al.*, 1989). A second example of such an application is the resolution of spatial and temporal variations of the magnetopause reconnection rate (which give cusp ion "steps" in satellite data) by using simultaneous incoherent scatter observations (*Lockwood et al.*, 1993a, *Lockwood*, 1995a). A related study by *Pinnock et al.* (1993) showed that the region of cusp precipitation, as seen by a low-altitude satellite, was co-incident with a longitudinal flow channel seen by an HF backscatter radar: longitudinal flows were also detected by the satellite, but only the radar could resolve that this flow channel was elongated and that it was one of a sequence of transient flow events. Both transient longitudinal flow channels and cusp ion steps are predicted ionospheric signatures of magnetopause reconnection bursts (i.e., flux transfer events or FTEs): the flow channels are expected when the magnitude of the dawn/dusk component of the magnetosheath field is large, the cusp ion steps will be more common when it is small. Such predictions for these, and other, transient events will be ideally tested by combined ground-based observations of the cusp ionosphere while Cluster is at the dayside magnetopause or crossing the dayside auroral oval.

(ii) Placing satellite observations in context

We can also use ground-based observations to place the Cluster observations in context, in both time and space. For example, ground-based data can be used to define boundaries (e.g.

convection reversal boundaries, the auroral electrojets, the locations of arcs, the zero potential contour between flow cells) which can give information about which regions of the magnetosphere-ionosphere system the spacecraft were in. In addition sequences of changes, for example during substorms, can be monitored from the ground. Thus ground-based data can be used to define where both events and spatial structures, seen by spacecraft, were in both time and space. An example of placing a spatial structure in context of the larger-scale spatial distribution is the recent work on the dayside field-aligned currents and magnetosheathlike plasma precipitations by *de la Beaujardiere et al.* (1992). They used radar observations of the convection pattern to resolve an ambiguity of which convection cell a satellite passed through. Likewise, ground-based data can determine when a feature was seen by a satellite in a sequence of events. This is particularly important for studies of the evolution of the magnetosphere-ionosphere system during substorms. *Opgenoorth et al.* (1989) employed ground-based data to investigate the evolution of a westward-travelling surge and showed that the satellite data were within the surge head which had recently ceased moving. *Pellinen et al.* (1992) used ground-based data with auroral images from satellites to show that the recovery phase is much more complex than a simple global return to quiet conditions.

Using ground-based data to place satellite measurements in a sequence of events has sometimes produced results which appear to conflict with the conclusions of other studies, which place them in a certain region of the magnetosphere-ionosphere system. There is much to be gained from resolving such conflicting evidence. For example, a major question in recent substorm research has been when and where substorm onset is located and, a related question, when and where the open lobe flux built up in the growth phase is destroyed by tail reconnection. *McPherron et al.* (1993) used ground-based observations of substorm onset to show that tail lobe field strengths begin to decay at onset, implying that enhanced tail reconnection causes onset and that the poleward expansion of the aurora is due to the closure of open flux. On the other hand, *Lopez et al.* (1993) compared particle and field data from the tail plasma sheet with observations by ground magnetometers and auroral imagers and have provided evidence that the tailward expansion of activity in the near-Earth tail is related to the poleward expansion of the aurora, implying onset is Earthward of, and before, significant closure of open flux by tail reconnection. It is clear that the resolution of these conflicting observations, and of this general debate between the "classical near-Earth neutral line" and "Kiruna conjecture" models, will require combinations of ground-based and satellite data (see review by *Lockwood*, 1995b).

(iii) Providing boundary conditions

The ionosphere is not just a passive mirror of magnetospheric processes, but an active part of a genuinely coupled system. In modelling the magnetospheric observations, it is vital to know the prevailing boundary conditions in the ionosphere. In particular, ionospheric conductivities are of importance and can be derived from altitude profiles from incoherent scatter radars or by comparison of electric and magnetic field values (e.g. *Kirkwood et al.*, 1988; *Buchert et al.*, 1988; *Brekke et al.*, 1989; *Kirkwood*, 1992). Observed conductivities can be used in a wide variety of ways to add crucial information to a number of studies. These include: studying Alfvén wave reflection at the ionosphere, for example in TCV events (*Glaßmeier*, 1992); testing theories of magnetosphere-ionosphere interaction, for example in

substorms (*Kan*, 1993) and, in particular, using numerical models (*Hesse and Birn*, 1991); calculating inductive time-constants for non-steady convection (*Sanchez et al.*, 1991); estimating ohmic heat dissipation (*Foster et al.*, 1983; *Heelis and Coley*, 1988; *Weiss et al.*, 1992) and deriving snapshots of the convection pattern by magnetometer inversion techniques (*Richmond*, 1992; *Knipp et al.*, 1993).

(iv) Quantitative estimates from combined data

Ground-based data can also be used with satellite data to gain information which cannot be obtained from either on their own. Obvious examples of this type of application would include the recognition of structures and sequences of events such that the mapping of convection-dispersed particle populations, waves, magnetic and electric fields from the magnetosphere to the ionosphere is revealed (for example, *Elphic et al.*, 1990). However, there are other less obvious applications: *Lockwood et al.* (1993a) have recently used a combination of satellite and radar data to compute the distance from the magnetopause reconnection site to the satellite. This measurement is not possible from either of the two data sets in isolation. Another example is the comparison of electron spectra seen at a satellite with that inferred at low altitudes on the same field line by an IS radar, giving evidence for field-aligned particle acceleration at heights between the two (*Kirkwood et al.*, 1989; *Kirkwood and Eliasson*, 1990).

2. Planning Procedures

In order to plan coordinated observations using Cluster and ground-based facilities, the European Space Agency ESA established a working group (*Opgenoorth*, 1993) for which two of the authors act as chairman (HJO) and the representative for incoherent scatter facilities (ML). The working group has met several times and organised a workshop in Orleans, France in March 1994, with a second to be held in Frascati in April 1995. As an initial basis for planning, the working group has followed ESA's Cluster Science Plan by classifying the orbits, such that apogee falls into one of four magnetic local time (MLT) sectors, namely 6 hours around 0 MLT, 6 MLT, 12 MLT and 18 MLT (i.e. the midnight, dawn, noon and dusk sectors). We also consider the ground-based station or meridian chain of stations to be simultaneously in one of the same four MLT sectors, which divides the possibilities into a total of 16 combinations. For each of the 16 there are a number of points on the Cluster orbit near which coordinated observations with a certain ground observatory are of special scientific interest. Thus far, we have defined 67 such conjunctions and configurations. Note that in this paper, we refer to "configurations" between any one ground-based observatory and the group of four Cluster craft: this should not be confused with the configurations of the four craft, relative to each other, which is variable and an important and complex part of the operations planning for the Cluster mission (*Rodriguez-Canabal et al.*, 1993). The numbers in figure 1 refer to those configurations/conjunctions which we have identified for periods when the Cluster orbit plane is close to the noon-midnight (GSE XZ) plane, whereas those in figure 2 are when the orbit plane is closer to the dawn-dusk (GSE YZ) plane. Figure 1 views the Earth and the Cluster orbit (thick line) from dusk and the small arrow shows the location of the ground-based observatory. The thin lines show a typical magnetopause location, along with geomagnetic field lines which thread the dayside low-latitude boundary layer (LLBL), the

high latitude boundary layer (HLBL or mantle) and the tail neutral sheet. Figure 2 views the Earth and the Cluster orbit from the sun and the thin lines show a typical magnetopause and field lines which pass through the low-latitude boundary layer on the dawn and dusk flanks of the magnetosphere.

To understand what is meant here by a configuration, consider the segment of the orbit marked 1 in the top left part of figure 1. For this configuration, the satellites are near apogee in the central current sheet of the tail, while the ground-based station in question makes observations of the midnight sector auroral oval. This is an example of a near-conjugate configuration. However, we also consider many non-conjugate configurations to be important. Configuration 2, on the same plot, is one such case, allowing ground-based observations of the development of the substorm aurora and electrojets in the midnight sector while Cluster makes simultaneous observations in the tail lobe. In figures 1 and 2 we label configurations where the ground-based observatory and Cluster are in opposite hemispheres with an asterix. In many of these cases, much of the same science can be addressed as when the two are in the same hemisphere; however, the interpretation of such data is often likely to be more difficult and, unless there are specific reasons to the contrary, the opposite-hemisphere configurations are considered to be of lower priority. However, we note that in cases where the satellite and radar data can be considered to be of similar type and quality, we may sometimes be able to use opposite-hemisphere observations to test for conjugate and non-conjugate phenomena (e.g. *Greenwald et al.*, 1990; *Rodger et al.*, 1994b).

We have made an initial assessment of a comprehensive list of potential scientific objectives for each numbered conjunction/configuration, as given in Table 1. The lists of characters refer to scientific objectives and areas of study toward which the combination of the ground-based observatory and Cluster is expected to make a significant and unique contribution. Table 2 is a key to these characters: lower case arabic characters are areas of study concerned with one of the major objectives of the Cluster mission, namely substorms; upper case arabic characters refer to more general areas of magnetospheric topology, dynamics and morphology; and greek characters refer to studies of the magnetopause boundary layers, including the other major Cluster objective, the cusp.

As will be discussed in section 4, some configuration/conjunctions are likely to occur (within 3-hour MLT tolerances) just 3 or 4 times per year. Others, particularly with the satellites near apogee, will be more common. Nevertheless, the large number of possible configurations leads to a great many opportunities for combined observations. In many cases, a great many more than we will be able to exploit. If, for example, we required an average of 6 hours EISCAT/ESR measurements for each of the 102 configurations of these radars with Cluster (including those with Cluster in the opposite hemisphere) shown in figures 1 and 2, we would require (6 x 3 x 102) = 1836 hours of radar operations in one year, even if we only take the best 3 occurrences. Given that for nearly all the scientific objectives it is highly desirable that the ESR operate simultaneously with both the EISCAT UHF and the VHF systems, only a fraction of this total number of operating hours will be achievable. In addition, the 4 Cluster craft will only be able to take data for an average of about 50% of each orbit, due to tracking limitations and on-board recording capacity. Hence for planning (both from the point of view of ground-based facilities and the Cluster Science Working Team, SWT), it is necessary to prioritise these possibilities. Table 1 also gives our initial assessment of the priorities, by selecting those that we see as very high priority (VHP) and high priority (HP).

These lists are still under discussion by the working group and will be extended and amended as the planning proceeds. In order to achieve this, an interactive implementation of figures 1 and 2 and Tables 1 and 2 can be accessed via the World-Wide Web (WWW), as will be discussed further in section 5. These pages allow suggested corrections and additions to be logged and the staff of World Data Centre C1 at RAL will maintain, correct and update the list after consultation with the relevant working group members. Hence this implementation provides a way for the world-wide community of ground-based researchers to refine and extend these planning options and adjust the priority ratings.

These WWW pages also give information on when any one of the conjunctions or configurations shown in figures 1 and 2 will occur, for any user-specified ground-based observatory. This information is based on the most recent orbital data from the Cluster Joint Science Operations Centre (JSOC) at RAL (*Dunford et al.*, 1993) and makes use of the Altitude Adjusted Corrected Geomagnetic Coordinates (AACGM) system and software (*Gustafsson et al.*, 1992; *Baker and Wing*, 1989). Prior to launch, the exact Cluster orbit is unknown and the predictions will only be valuable for testing various operational scenarios and software. However, the predictions are regenerated with each user request and, after launch, will always be based on the most recent information and the same orbit predictions as used by the JSOC for planning Cluster operations. We will receive various data from the JSOC once per week. From this we will compile the list of events (for example magnetopause crossings, see section 5) which are the basis of the predictions which can be obtained via these pages. There will be five classes of orbit and operations predictions for any date and UT (time t):

T. Pre-launch test scenario data (code T for test)
I. Initial plans at t - 6 months (code I for initial)
R. Refined plans at t - 4 months (code R for refined)
A. Agreed plans at t - 2.5 months (code A for agreed)
F. Final plans at t - 2 weeks (code F for final)

The refined (R) plans may differ from the initial plans (I) because of orbit manoeuvres and will form the basis of Cluster Science Working Team discussions, held roughly every 3 months. The result of these discussions are the agreed plans (A), to which JSOC will only make minor adjustments to meet operational constraints, before the final plans (F) are approved by the project scientist and transmitted to the spacecraft. For any one configuration with a certain ground observatory site, the predictions given will always be the most up to date, and will carry the T, I, R, A, or F status flag.

In addition, we hope to arrange a fifth classification with JSOC:

P. Post-observation data at t + 1 month (code P for post)

These will be very useful in exploiting the data after they are acquired.

The WWW pages will also allow ground-based experimenters to record their most recent plans for observation times and modes, based on these predictions, which will be automatically passed on to JSOC. The T, I and R predictions will enable us to make provisional plans for our ground-based facilities. These will be used by HJO at Cluster SWT

meetings to try to ensure that Cluster data are, wherever possible, taken in the desired modes (normal or burst) at the desired segment of the orbit, with the four satellites in the desired constellation and orientation. The A and F plans will allow us to, respectively, decide upon and finalise our operating schedules but are for information only: it is extremely unlikely that we will be able to influence the Cluster data-taking strategy after t - 3 months, and the earlier we know of the provisional plans for the ground-based facility, the more chance there is of accommodating them with those of SWT and JSOC.

3. Examples of Very High Priority Cases

The permutations of science topics and satellite-ground configurations listed in Table 1 are far too numerous to explain here in detail. However, to illustrate the choice of scientific objectives and the priorities, we here explain our thinking for just two cases. We chose configuration 1, one of the most important of many novel possibilities for substorm studies, and configuration 5, which will give extremely exciting new studies of the dayside boundary layers and cusp. These two cases exemplify the kind of arguments and thinking we have used in the compilation of Table 1.

(i) Studies of nightside magnetospheric disturbances and substorms using configuration 1

Even during times of extreme magnetic quiescence, often associated with northward IMF conditions, the magnetosphere does not remain undisturbed. *Kamide et al.* (1975, 1977) and *Lui et al.* (1976) have shown that substorm-like magnetic activity can occur, even on a highly contracted auroral oval. The links between these disturbances and magnetospheric processes are still not understood and possible differences from ordinary substorms are of interest. We require observations of the contracted oval, by stations and radars with a field-of-view at very high-latitudes, along with simultaneous Cluster measurements in the tail lobe or plasma sheet (configurations 2 and 1, respectively). (For these reasons, scientific objectives w, J, o and v from Table 2 are among those listed in Table 1 for configuration 1 of Cluster with the ground-based facilities).

Other features of the relatively quiet magnetosphere are the so-called "theta" auroras and other sun-aligned arcs (*Murphree and Cogger*, 1981; *Frank et al.*, 1982; *Murphree et al.*, 1989) and auroral structures within the polar cap, such as in the "teardrop" or "horse-collar" aurora (*Hones et al.*, 1989). Such features are out of reach for most ground-based auroral zone instrumentation and so their dynamics and possible links to magnetospheric regions and processes have remained a puzzle. They appear to occur during periods of northward-directed IMF (*Elphinstone et al.*, 1990), and hence our relative ignorance of these phenomena is despite the fact that they are associated with a magnetospheric configuration which prevails for 50% of the time. *Pellinen et al.* (1990) have shown that the dynamics of transpolar arcs involve substorm like features, and detailed studies will be possible with the new ESR and SUPERDARN radars as well as Sondrestromfjord and EISCAT. Understanding the possible underlying magnetospheric processes and topology will be an important topic for Cluster studies in the magnetospheric tail lobes and plasma sheet (scientific objectives G, o, A, B, C, D, G, I, J).

The early development of a substorm is often characterized by equatorward-drifting auroral arcs, indicating enhanced magnetospheric energy storage. They are seen in the late growth

phase and early expansion phase, poleward of where onset will later occur or has already occurred, respectively. The origin of these arcs is still not completely understood, but there is some evidence that they are associated with Earthward-moving structures within the plasma sheet boundary layer and the central plasma sheet, the northernmost arc being close to the open/closed field-line boundary (*de la Beaujardiere*, 1994, *Elphinstone et al.*, 1994). With a single satellite, it is hard to identify such structures, but they are clearly seen in auroral images and IS radar data and the combination of these ground-based facilities and the four Cluster satellites will be invaluable for the identification of the magnetospheric sources of these arcs and their associated field-aligned current systems. These multiple, equatorward-drifting arcs are of interest for several reasons. They are observed to be associated with considerable ionospheric ion outflows (*Wahlund et al.*, 1989; 1992), which could populate the near-Earth central plasma sheet with oxygen ions and influence substorm development there (scientific objective j). The equatorward drift motion was also observed to be unaffected by substorm onset at lower latitudes, at least until the poleward substorm expansion reaches their latitude and they are engulfed by the main substorm aurora. This agrees with the concept of substorm onset occurring in the near-Earth central plasma sheet location, such that the boundary plasma sheet (BPS) and plasma sheet boundary layer (PSBL) remain unaffected for at least for the first ten minutes of the expansion phase after onset (see *Persson et al.*, 1994a; b and *Gazey et al.*, 1994). Radar data also indicates that the conductivity they produce can be so large as to initially reduce the local ionospheric electric field to almost zero (*Morelli et al.*, 1995). Combined satellite ground observations will be essential to investigate both the origins and the effects of these equatorward-drifting arcs (scientific objectives i, j, m, q, r, t).

Recently, the scenario of the so-called "Kiruna Conjecture" of substorms (*Kennel*, 1992) has increasingly gained acceptance. This is because evidence has accumulated that substorm onset usually takes place around X = -8R_E, which is relatively close to the Earth in the central tail current sheet (see *Lui*, 1992, and references therein). This places substorm onset (and the pre-existing auroral oval) at the modelled location of the maximum cross-tail current strength (*Kaufmann*, 1987; *Pulkkinen et al.*, 1992). In contrast to this inferred near-Earth location of onset, signatures of reconnection (specifically the direction of accelerated plasma flows and the polarity of the magnetic field across the tail current sheet) place the near-Earth neutral line (NENL) somewhere beyond X= -20 R_E (*Baumjohann et al.*, 1991; *Baumjohann*, 1993). This conclusion is very important, because it means that the observed disruption of the cross-tail current at substorm onset is not co-located with the NENL but happens considerably Earthward of it. Important questions will then have to be raised as to whether the NENL gives rise to the current disruption, or vice versa (see review by *Lockwood*, 1995b). In configuration 1, Cluster will pass through the likely region of NENL formation but will, according to the Kiruna conjecture, see the substorm current disruption expanding tailward. The IS and HF radars, surrounding magnetometer arrays, and other ground-based instrumentation such as optical and riometer imagers, will allow us to monitor the onset and spreading of the current disruption, thereby addressing these key questions. It is crucial to understand when in the evolution of the substorm (as seen from the ground) do the signatures of tail reconnection (as seen by Cluster) commence, and to know when the NENL starts to reconnect open lobe flux, thereby detaching the plasmoid from the Earth (*Moldwin and Hughes*, 1992; *Slavin et al.*, 1992). Note that by the time that this pinching off takes place, the plasmoid may well be already moving down the tail (*Owen and Slavin*, 1992). *Opgenoorth et al.* (1994) have recently shown that there are clear auroral intensifications in even the later phases of substorm

development (in the recovery phase), and these may be associated with the relatively late detachment of a plasmoid. (scientific objectives a-f, h, i, l, v, B, I).

Ground-based data often show a substorm onset, which subsequently fails to develop into a full substorm (*Lui et al.*, 1976; *Untiedt et al.*, 1978; *Koskinen,* 1992). The behaviour of the tail current sheet and the reason for the incomplete substorm development is not yet known (scientific objective g). Similarly it can be shown, by combining ground-based and near-Earth satellite data sets, that during multiple substorm intensifications the appearance and strength of the disturbance does not always agree in the ionosphere and the near-Earth space (*Yeoman et al.,* 1994, *Grande et al.*, 1992, 1994). We believe that many questions concerning the individual substorm development and the causal sequence of events might be solvable by studying either incomplete substorms (pseudobreakups) or multiple-onset substorms with multipoint measurements in various regions of the ionosphere/magnetosphere system. While Cluster and other satellites study the tail variations during substorms, the radars and other ground-based instrumentation could study the ionospheric convection, precipitation and field-aligned currents, which transfer energy and momentum to the ionosphere (scientific objectives t and m), and monitor the dynamics of the various boundaries. A goal of particular importance is detecting and tracking the development of the open/closed field-line boundary (scientific objectives s and B), not only during the growth and recovery phases of individual substorms, but also during incomplete and multiple substorm intensifications, thus determining the relative importance in terms of magnetospheric energy release. Other more localized features in the early expansion and late recovery phase are the westward travelling surge and Omega bands which, from an auroral point of view, are the most dominant features in the evening and morning sectors, respectively. While their basic magnetospheric source regions for the features are identified, many questions about their exact mechanisms of formation and dynamic development are still open (see *Opgenoorth et al.*, 1989, 1994) (scientific objectives g, t, m, s, B, I).

There are other scientific questions, not specifically related to substorms, which the configuration 1 will allow us to study. High energy electrons follow trajectories which are close to field-aligned because the field lines onto which they are frozen do not convect far in their time of flight. These will be detected by Cluster and can be monitored by the radars from the low-altitude density enhancements they cause. Hence comparing the spatial distributions of high-energy electron precipitation seen by the Cluster craft and by the radars may tell us about how field lines map (scientific objective A) and comparing the derived energy spectra could, in principle, tell us about acceleration processes between the spacecraft and the ionosphere (scientific objective H). However, limitations in time and energy resolution of both data sets may not allow firm conclusions to be drawn. Induction effects mean we cannot assume that electric fields map to the ionosphere for short time scale phenomena (*Lockwood and Cowley*, 1992). For example, the sunward convection surge in the equatorial magnetosphere associated with field line dipolarisation appears not to have an ionospheric counterpart in electric fields. Simultaneous radar flow and Cluster observations can help to confirm this and allow measurement of the inductive smoothing time constant of the ionospheric flow. Such studies will also be important for understanding the ionospheric convection associated with bursty bulk flow events which appear to be responsible for most of the flux transport in the central plasma sheet (*Angelopolous et al.*, 1992a; b; *Sergeev et al.*, 1992). (scientific objective A).

(ii) Studies of dayside boundary layers, cusp and cleft using configuration 5

Much recent interest has focused on how and where reconnection takes place at the dayside magnetopause (see reviews by *Lockwood*, 1995a, and *Crooker and Toffeletto*, 1995). *Lockwood and Smith* (1994) have recently made predictions of the cusp ion dispersion signatures, as would be seen by the Cluster craft during mid-altitude cusp crossings, when the rate of reconnection at the dayside magnetopause is pulsed. The predicted poleward migration of the cusp ion steps (caused by the periods of low reconnection rate between pulses) should be detected by comparing the ion data from the different Cluster spacecraft. The theory predicts this motion to be associated with poleward-moving ionospheric electron temperature enhancements, 630 nm (red-line) auroral transients and transient bursts of longitudinal flow These have already been detected by EISCAT and optical instruments on Svalbard (*Lockwood et al.*, 1993a; *Sandholt et al.*, 1990). Not only do combined observations provide valuable confirmation of the theory of the effects of pulsed reconnection, but they allow the location of the reconnection site to be determined, as discussed in section (1-iv). Furthermore, the method of *Lockwood et al.* (1994) can be used to compute a variety of important parameters at the reconnection site which may well control the reconnection behaviour (including the local magnetosheath density, temperature, Alfvén speed and field strength, as well as its field-aligned flow speed). Thus the combined observations offer unique opportunities to study the causes of reconnection rate changes (scientific objectives α, Ω, π, β, γ, δ and ζ).

In addition, comparisons with simultaneous interplanetary measurements from the WIND and IMP-8 satellites will allow us to study the percentage of ions which are transmitted across the rotational discontinuity near the deduced reconnection site, as well as their consequent acceleration and any heating (objectives ε and Θ). Experimental estimates of the transmission factor have varied from 0.5 (*Fuselier et al.*, 1991) to 0.1 (*Onsager et al.*, 1994) and measurements of the distribution functions of the accelerated ion flows by *Smith and Rodgers* (1991) are in close quantitative and qualitative agreement with the predictions of *Cowley* (1982). The important dimension brought to these studies by the ground-based observations is the location of the X-line, for which the solar wind parameters can then be used to give first-order (gas-dynamic) estimates of the density and temperature of the magnetosheath plasma at the X line. A feature which urgently needs explanation is how quasi-neutrality is maintained, even though the injected electrons move so much faster than injected ions (objective η - see *Onsager et al.*, 1993). The lower density, higher average energy plasma seen on the most recently reconnected field lines (because of ion flight time effects) is almost certainly what is called the "cleft/LLBL" precipitation (*Newell et al.*, 1989; *Newell and Meng*, 1992). It is a question of recent debate as to whether there is also an LLBL on closed field lines (*Onsager et al.*, 1994) and, if so, where it is, how it is populated with sheath plasma and what voltage this mass transfer places across such a closed LLBL. The existence and occurrence of a closed LLBL can be evaluated by looking for LLBL-like precipitation on field lines whose motion and evolution, as seen by the radars, cannot be explained as newly-opened field lines (*Newell et al.*, 1991) (objectives θ and λ). In addition, "double" or "overlapping" injections have been seen in the higher density "cusp" precipitation (*Norberg et al.*, 1994). These pose interesting and challenging theoretical problems in terms of understanding how these particles are injected across the magnetosphere onto field lines which are convecting but are then dispersed according to their time of flight, such that two distinct populations are seen at one observation time (objectives Ξ and Ω).

Pulses of reconnection, between the geomagnetic field and an IMF with a large B_y component, have been invoked as a cause of transient flow bursts and coincident poleward-moving transient auroral events in the cusp/cleft ionosphere (*Sandholt et al.*, 1990; *Lockwood et al.* 1990, 1993b; *Pinnock et al.*, 1993). A key question about the predominantly red-line (630 nm) auroral events is the altitude at which they are produced, as this influences our estimates of the size of the events (*Lockwood et al.*, 1993b). The emission profiles of 630 nm light are determined by the altitude profiles of ionospheric electron density and temperature, both of which are enhanced by the precipitating magnetosheath plasma in the cusp region. In addition, the transient patches of 630 nm emission are associated with small regions of dominant 557.7 nm (green-line) emission. These are known to be coincident with the upward field-aligned current of the oppositely directed matched pair which transmit the longitudinal motion into the ionosphere (*Sandholt et al.*, 1990; *Lockwood et al.*, 1993b.). However, the causes of the required electron acceleration are not known. The ESR will be ideal for studying these processes and the emission profiles because Svalbard offers optical observations of the cusp in darkness. In particular, if reconnection pulses are confirmed to be the origin of poleward-moving events in the radar data, it becomes crucial to measure their area because this gives an estimate of the total flux opened by each reconnection pulse, and hence the contribution to the average transpolar voltage (objectives μ,ξ - see *Lockwood et al.*, 1990). The pulsed nature of reconnection has been invoked in a variety of ways as a part of suggested mechanisms for the production of polar cap density patches (e.g. *Rodger et al.*, 1994a). These hypotheses could be tested if ground-based facilities were used to detect the patches and monitor their formation, while the Cluster observations of the cusp ion dispersion characteristics were used to evaluate the reconnection behaviour (objective Σ). The flow bursts observed by EISCAT must be associated with transient enhancements of dayside field-aligned currents but the temporal evolution of the distribution of dayside field-aligned current caused by reconnection pulses have not yet been studied (objective Δ).

A major complication is that transient flows, aurorae and field-aligned currents are also key features of travelling convection vortices (TCV's) (*Friis-Christensen et al.*, 1988; *Glaßmeier et al.*, 1989). These are thought to result from solar wind pressure pulses but a variety of different mechanisms have been proposed (*Kivelson and Southwood*, 1989; *Lysak and Lee*, 1992). Thus the origin, propagation and lifetime of TCVs are still not known. In addition, they appear to be associated with soft precipitation equatorward of the background cusp/cleft (*Heikkila et al.*, 1989, *Potemra et al.*, 1992, *Jacobsen et al.*, 1989, *Lühr et al.*, 1995) which is not predicted by the current theories of their generation (objectives Λ and σ).

As on the nightside, magnetic mapping is uncertain in the cusp/cleft region, and in addition is likely to be highly dependent on the amount of open flux threading the dayside magnetopause (*Crooker et al.*, 1991, *Crooker and Tofelletto*, 1995). Induction effects mean that the voltage pulses (i.e. flux transfer events) in the magnetopause are decoupled from the ionosphere where they cause only smoothed poleward flow unless the magnetosheath B_y component is large (see review by *Lockwood* 1995a). Comparisons between radar flow observations and Cluster data, when in close conjunction in the cusp/cleft region will help answer the vexed questions of how both magnetopause magnetic and electric fields map into the ionosphere (objective A). Much attention has been given to the cusp when the IMF is southward and relatively little to its behaviour when it is northward, which can often be complex (e.g. *Weiss et al.*, 1995). Configuration 5 would be valuable for studying how the

northward IMF cusp relates to transpolar arcs and sunward convection in the lobe (objectives J and G).

Lastly, the cusp/cleft region is known to be a major source of ionospheric plasma for the polar magnetosphere in the cleft ion fountain (*Lockwood et al.*, 1985). The IS radars and digital ionosondes could be used to detect the upflows in the cusp ionosphere while the Cluster spacecraft observe them in the dayside auroral oval and their dispersion by convection into the near-Earth lobe. Thus the combined Cluster-ground-based data can yield information about the location and causes of the cleft ion fountain (objective τ).

4. An operations scenario

At the time of writing, the exact Cluster orbit is unknown and hence neither are the UT at which the spacecraft are in any one location. As it is this UT which determines the location of a ground-based facility, this information is vital for planning coordinated measurements with any one ground-based observatory. Consequently, detailed plans cannot yet be made. However, to gain an idea for the likely operating schedules we here consider the nominal Cluster orbit of 57 hours (i.e. 2 days 9 hours). Table 3 considers the evolution of the relative locations of the satellites and one ground-based station, following an ideal occurrence of just one configuration (the example chosen here is number 5) from the list given in Table 1. This conjunction is said to be ideal if the satellites are at noon when crossing the dayside auroral oval, and ground observatory is also at magnetic noon (which is at a UT of roughly 9 hrs at Svalbard). This can be seen to be the case for orbit 1 because the difference in longitude between the ideal and actual radar sites, δL, is zero; as is the difference between the ideal and actual MLT of the satellite, δMLT. At the same point of the next orbit (2), the radar location is far from ideal, with δL = 9 hrs. For orbit 3, δL is -6 hrs when Cluster is in the interior cusp. Note that although this is not a usable occurrence of the (very high priority) configuration 5, satellite data on the cusp could still be of use because it is an ideal occurrence of configuration 8 (high priority). Orbit 5 gives a configuration 3 when Cluster is in the interior cusp but, as shown by Table 1, this is considered a low priority. The interior cusp crossing on orbit 7 yields configuration 12 (high priority) and configuration 5 is regained on orbit 9. Note, however, that in this 8-orbit cycle, the satellite has drifted by 1.25 hrs of MLT (because the satellite orbit plane moves through 0.156 hours of MLT per orbit, covering 24 hours in a year). If, for example, we wish the satellite to be within 2 hours of the ideal ($|\delta MLT| < 2$ hours) for any one configuration, we will only have 2 or 3 occurrences per year of the mission. Note that the planning pages allow the user to specify the maximum $|\delta L|$ which is acceptable. The limit on $|\delta MLT|$ is set to 3 hrs, consistent with the idea of sorting of the ground-based station location into one of the four MLT sectors.

A corresponding analysis can be applied to each of the configurations/conjunctions which occur with Cluster at other points of the orbit. The key point for operations planning is that different ideal configurations will occur during the same orbits. For example, the (very high priority) configuration 1 requires Tromso at 24 MLT, so that the satellites are at apogee in the tail at about 21:30 UT. This is roughly achieved during orbit 2 in Table 3 on day 4 at 23:30 UT (so δL = 2 hrs) and during orbit 7 on day 16 at 20:30 UT (δL = -1 hr). Other important configurations will also occur in the same period. The complexity of the planning is yet further increased by the choices for operations made by the Cluster SWT, their selection

of data-gathering periods, satellite separation strategy and the instrument modes.

The World-Wide Web pages compile for the user a list of the predicted occurrences of one or more of the configurations for a user-specified ground-based observatory, to within a $|\delta L|$ tolerance which is also set by the user. How to make use of these pages is described in the following section.

5. Using the Planning Procedure on World Wide Web

The planning procedure is based on some pages on World Wide Web (WWW: the URL is http://wdcc1b.bnsc.rl.ac.uk/). To make full use of these pages, an image-handling browser such as Mosaic is needed. These pages were installed in September, 1994 and have been, and will continue to be, refined on the basis of user feedback.

These pages allow you to gain information about any one, or any combination, of the configurations/conjunctions listed in Table 1, in that for each they will give a list of potential scientific objectives and of the predicted date and UT of each occurrence. In addition, selecting any of the list of potential objectives in table 2 will give a list of all the configurations which may be of relevance. The configurations/conjunctions are given the same numbers as in Table 1 and can be selected by that number or from implementations of figures 1 and 2, each number on the plot being an active "hot link" to the information.

At various places, the pages offer you predictions of the orbit, based on the JSOC orbital and operations data. The user then has to select which ground-based facility he wishes predictions for: some of the major facilities are stored in a pull-down menu, but the user can enter any other (the name and geographic coordinates are all that is required). The user also sets the tolerance of $|\delta L|$, specifying how close the conjunctions he is interested in. The configuration(s) he is interested in can then be selected, either via the implementations of figures 1 and 2, or by entering the number or numbers or even the priority rating or ratings.

The software then generates a list of the occurrences of the selected configuration(s) in chronological order. An example for the configuration 1 (as discussed in section 3-i) is presented in Table 4 and for configuration 5 (as discussed in section 3-ii) is given in Table 5. In both cases the site selected was the EISCAT site at Tromsø. For configuration 5, the conjunctions are only valuable if the ground observatory is within, at most, 3 hrs in MLT of the satellite at the time of the cusp/cleft crossing and hence the maximum $|\delta L|$ was set at the (default) value of 3 hours. In fact, the (shorter) lists for $|\delta L| < 6$ hrs. will always contain a few occurrences which $|\delta L|$ is greater than the maximum requested, these being cases when both satellite and ground facility are within the relevant 6-hour MLT sector. These are included in the lists because several users noted that interesting passes were often overlooked if a rigid $|\delta L|$ criterion was applied.

In Table 4, the maximum $|\delta L|$ was set to 10 hours. This is because the satellite spends a much greater time near apogee, where it is required for configuration 1. Thus Cluster remains close to the required location for a longer period, giving the ground observatory more chance of rotating with the Earth into the required location. Hence there is a greater range of $|\delta L|$ which we can employ, δL being evaluated for each site at the UT when the satellite is in the ideal location. Thus configurations near apogee, like 1, will be much more common than those near

perigee (like 5) and this is reflected in the relative lengths of tables 4 and 5 (although this is in part due to Table 4 giving the occurrences of Cluster apogees as well as the predicted neutral sheet crossings).

Notice that selection of 1 and 5 together would give a list of the occurrences of both, interleaved in chronological order. There is no limit to the number of different configurations/conjunctions which can be included in any one list of predictions. For example, Table 6 shows the listings for the EISCAT Tromsø site, using the option to select VHP (very high priority) cases only. This example gives an indication of the likely scheduling requirements for any one ground-based observatory.

The first column of tables 4-6 refer to the location of Cluster. The arrival of Cluster at each location is called an "event", as discussed further below. Each entry in this column is a hot-link to plots which will show how the four craft will be configured at that time, and plots of the whole orbit, marked with the segments where data taking is planned. (Note that these plots will only be available after launch, i.e. for the I, R, A, F and P status predictions). The second and third columns give the date and UT of the predicted occurrence of the required configuration, and the next two columns give the MLT of Cluster and of the ground station, at that time. The next column tells us how far the ground station MLT is from the ideal value for that configuration, δL. The third from last column gives the status of the orbital data used in the prediction. At present, only test (T) data are available. During the mission, the entries at the top of the table will be P, but these will change through the sequence F, A, R, and I, with the prediction furthest into the future remaining only at T status. The last two columns give the configuration number and a reminder of its priority.

The coding used for the Cluster "events" is illustrated by figure 3. This example of a Cluster orbit has apogee at noon. (Notice that figure 3 views the Earth from dawn and hence the sunward (positive X) direction is to the right: figure 1, on the other hand, views the Earth from dusk and the sunward direction is thus to the left of each plot). The present orbit plan is for the craft to move southward at perigee and the sequence of events predicted for one orbit is:

PE_###	- perigee
AO_###_S	- southern auroral oval intersection (including cusp/cleft near 12 MLT)
LO_###_S	- centre of southern lobe transition
MP_###_S	- magnetopause intersection in the southern hemisphere
BS_###_S	- bow shock intersection in the southern hemisphere
AP_###	- satellite apogee
BS_###_N	- bow shock intersection in the northern hemisphere
MP_###_N	- magnetopause intersection in the northern hemisphere
LO_###_N	- centre of northern lobe transition
AO_###_N	- northern auroral oval intersection (including cusp/cleft near 12 MLT)

Other orbits with the Cluster apogee in the tail will have no magnetopause nor bow-shock crossings, but instead will have:

NS_###	- tail neutral sheet

In all cases ### is the orbit number, which applies from one perigee to the next.

Magnetopause locations are predicted for median interplanetary conditions. Lobe centre times are midway in time between the auroral oval and magnetopause crossings, unless the latter do not exist, in which case lobe centre times are midway between the auroral oval intersection and the tail neutral sheet crossing.

The tick marks on the orbit shown in figure 3 are one hour apart. Note that the craft are close to "events" near apogee for extended periods, making the configuration with the ground-based station more likely to occur at some UT. For the orbit shown in figure 3 with, for example, a ground-based observatory at noon in the northern auroral oval, figure 1 (second plot of lower row) shows the configuration numbers are: 21 (AP), 22 (MP_N), 23 (LO_N), 24 (AO_N), 25 (PE), 24* (AO_S), 23* (LO_S), and 22* (MP_S). (See figures 1 and 2).

However, we do not intend that these pages only be a tool for providing information about where Cluster is predicted to be and when favourable configuration occur. The problem is that there are a great many variables concerning Cluster operations. Arguably the most important is the segments of the orbit for which Cluster will take data: there is little point in planning conjunctions with spacecraft which are not taking any data! However, in addition there are instrument modes and the 4-craft constellation form to consider. The Chairman of the Working Group (HJO) is a member of the Cluster Science Working Team (SWT) and will be able to advocate certain observation periods in certain modes where special opportunities exist for co-ordination with ground-based observatories. However, he can only carry out this task if he knows the wishes of the ground-based community in advance. The pages presented here will be the way to input your plans and requests via a form page. These we will sort, reply to and confirm by e-mail and then pass on to HJO and JSOC. Please note that for us to be able to sort the inputs and update your plans we will need all ground-based experimenters to register, which can also be done via a form on the web pages. After launch, the I, R, A, F and P predictions will only be available to those scientists who have registered.

A crude representation of how the planning cycle will work is given in figure 4. This plot shows the flow of various pieces of information between the Cluster Operation Centre (JSOC), the Ground-Based Data Centre (GBDC, hosted by the WDC-C1 for STP at RAL), the Chairman of the Working Group (HJO) and the Cluster Science Working Team (SWT). The solid arrows are information flow about Cluster operations plans, and cover the prediction status classes given by the solid letters. The dashed arrows are the information flow about the ground-based operations, covering the status classes given by the open characters. Ground-Based (GB) observers will receive the latest predictions from JSOC, via the GBDC using the WWW pages described here. They will also input their plans and wishes via these same pages. These will be updated and sorted by GBDC and the initial and refined (I and R) plans passed on to HJO who will inform SWT and, wherever possible, will argue for suitable Cluster data taking. The SWT will generate the Approved (A) plans which JSOC will turn into the final operations plan which are sent to the project scientist before transmission to the satellites. The GBDC will also keep JSOC informed of the plans of the ground-based community.

It is very important to note that Cluster operations can only be influenced via the GBDC and thence the SWT. In addition, after the SWT meeting, it will not be possible to further

influence the A and F plans. The representative for the GB community on SWT (HJO) will argue to maintain the elements of the R plans which GB scientists have noted as favourable. He will also lobby to change unfavourable plans, particularly when rare and important opportunities would otherwise be missed. The operations planning for the four Cluster craft is extremely complex and cannot be discussed properly here. However, there is flexibility which can be exploited. For example, planning is done in groups of three orbits and it is hoped that the plans for one whole orbit can be swapped with those for another in the same group of three. However, a key point is this: the sooner we know the wishes of the GB community for special orbits, the more chance we have of ensuring that the Cluster data taking is appropriate. After about 3 months before the pass in question there will be no chance for further changes. It is therefore vital that the GB community remain aware of the predicted orbit for many months in advance. This will be possible with the system which is now in place, as has been described here.

6. Conclusions

We have outlined a procedure whereby ground-based observations can be planned so as to support the Cluster mission to maximum effect. We have also briefly reviewed some past combined satellite and ground observations and suggested objectives to stimulate thinking about the variety of measurements which could be carried out. This review is far from complete, but examples have been selected to illustrate the range of uses of ground-based data and the potential to support Cluster observations. It should be noted that Table 1 contains many examples which do not rely on (even approximate) magnetic conjugacy between the satellites and the ground observatory.

The planning is not only required for the ground-based observations: it is vital that we are able to input the wishes of the ground-based community into the Cluster operations planning cycle at the earliest possible opportunity. The World Wide Web pages provide a simple way for the community to view current orbit predictions and operational plans and to input their own wishes. We urge all users and operators of ground-based facilities to familiarise themselves with them in advance of the Cluster launch.

Acknowledgements. We are grateful to M.A. Hapgood, project scientist of the Cluster JSOC at RAL, for assistance in establishing the required interfaces with JSOC. The procedure presented here was first presented at the Japan-EISCAT Symposium on the Polar Ionosphere (JESPI), held in Toba in August/September 1994. We thank the staff of the Solar-Terrestrial Environment Laboratory, Nagoya and the staff of the EISCAT Scientific Association for organising JESPI and to STEL for support for ML and HJO to attend the meeting. We are grateful to the other members of the ESA Cluster Ground-Based Working Group for many discussions and to J-P Villain for the local organisation of the Orleans workshop.

7. References

Angelopoulos, V., W. Baumjohann, C.F. Kennel, F.V. Coroniti, M.G. Kivelson, R.Pellat, R.J. Walker, H. Lühr and G. Paschmann, Bursty bulk flows in the inner central plasma sheet, *J. Geophys. Res.*, ***97***, 4027-4039, 1992a.

Angelopoulos, V., C.F. Kennel, F.V. Coroniti, R. Pellat, M.G. Kivelson, R.J. Walker, W. Baumjohann, G. Paschmann, and H. Lühr, Bursty bulk flows in the inner central plasma sheet: an effective means of earthward transport in the magnetotail, *in Proceedings of the First International Conference on Substorms, (ICS-1)*, Kiruna, Sweden, March 1992, *ESA-SP-335*, pp. 303-308, 1992b.

Baker, K.B. and S. Wing, A new magnetic coordinate system for conjugate studies at high latitudes, *J. Geophys. Res., 94*, 9139-9143, 1989.

Balogh, A., S.W.H. Cowley, M.W. Dunlop, D.J. Southwood, J.G. Tomlinson, K.-H. Glaßmeier, G. Musmann, H. Lühr, M.H. Acuňa, D.H. Fairfiel, J.A. Slavin, W. Riedler, K. Schwingenschuh, F.M. Neubauer, M.G. Kivelson. R.C. Elphic, F. Primdahl, A. Roux and B.T. Tsurutani, The Cluster magnetic field investigation: scientific objectives and instrumentation, in *Cluster: mission, payload and supporting activities, ESA-SP-1159*, pp. 95-114, 1993.

Baumjohann, W., The near-Earth plasma sheet, an Ampte/IRM perspective, *Space Sci. Rev.*, 64, 141-163, 1993

Baumjohann, W., G. Paschmann, T. Nagai, and H. Lühr, Superposed epoch analysis of the substorm plasma sheet, *J. Geophys. Res.*, ***96***, 11,605-11,608, 1991.

Brekke, A., C. Hall, and T. L. Hansen, Auroral ionospheric conductances during disturbed conditions, *Ann. Geophys., 7*, 269-280, 1989

Buchert, S., W. Baumjohann, G. Haerendel, C. La Hoz, and H. Lühr, Magnetometer and incoherent scatter observations of an intense Ps 6 pulsation event, *J. Atmos. Terr. Phys.*, 50, 357-367, 1988

Cowley, S. W. H., The causes of convection in the Earth's magnetosphere: A review of developments during IMS, *Rev. Geophys., 20*, 531-565, 1982.

Cowley, S.W.H., A. P. Van Eyken, F. C. Thomas, D.J.S. Williams, and D. M. Willis, The scientific and technical case for a polar cap radar, *J. Atmos. Terr. Phys., 52*, 645, 1990.

Crooker N.U., and F.R. Toffoletto, in *"Physics of the magnetopause"*, ed. B.U.O. Sonnerup, Proc. Chapman Conf. on the Magnetopause, American Geophysical Union Monograph, in press, 1995.

Crooker N.U., F.R. Toffoletto, and M.S. Gussenhoven, Opening the cusp, *J. Geophys. Res.*, ***96***, 3497-3503, 1991b.

de la Beaujardiere O., P.T. Newell, and R. Rich, Relationship between Birkeland current regions, particle participation, and electric fields, *J. Geophys. Res.*, ***98***, 7711-7720, 1993.

de la Beaujardiere, O., L. R.Lyons, J. M. Ruohoniemi, E. Friis-Christensen, C. Danielsen, F. J. Rich, and P. T. Newell, Quiet time intensifications along the poleward auroral boundary near midnight, *J. Geophys. Res.*, in press, 1994

Denig, W.F., W.J. Burke, N.C. Maynard, F.J. Rich, B. Jacobsen, P.E. Sandholt, A. Egeland, S.Leontjev, and V.G. Vorobjev, Ionospheric signatures of dayside magnetopause transients: a case study using satellite and ground measurements, *J. Geophys. Res.*, ***98***, 5969-5980, 1993.

Dunford, E., P. Vaughan, E. Golton, and T. Dimbylow, The Cluster Joint Operations Centre, in *Cluster: mission, payload and supporting activities, ESA-SP-1159*, pp. 291-298, 1993.

Elphic, R.C., M. Lockwood, S.W.H. Cowley, and P.E. Sandholt, Flux transfer events at the magnetopause and in the ionosphere, *Geophys. Res. Lett., 17,* 2241-2244, 1990.

Elphinstone, R.D., K. Jankowska, J.S. Murphree, and L.L. Cogger, The configuration of the northern auroral distribution for interplanetary magnetic field B_z northward, 1. IMF B_z and B_y dependencies as observed by the Viking satellite, *J. Geophys. Res.*, ***95***, 7591, 1990.

Elphinstone, R. D., D. J. Hearn, L. L. Cogger, I. Sandahl, D.M. Klumpar, and M.Shapshak, The double oval UV auroral distribution: Implications for the substorm process, in *Proceedings of the International Conference on Substorms (ICS-2)*, in Fairbanks, USA, March 1994, in press, 1994

Foster, J.C. et al., Joule Heating at high latitudes, *J. Geophys. Res., 88*, 4885, 1983.

Frank, L. A., J. Craven, J. L.Burch, and J. D. Winningham, Polar views of the Earth's aurora with dynamics explorer, *Geophys. Res. Lett., 9,* 1001-1004, 1982

Fuselier, S.A., D.M. Klumpar, and E.G. Shelley, Ion reflection and transmission during reconnection at the earth's subsolar magnetopause, *Geophys. Res. Lett.*, ***18***, 139-142, 1991.

Friis-Christensen, E., M.A. McHenry, C.R. Clauer, and S. Vennerstrom, Ionospheric travelling convection vortices observed near the polar cleft: A triggered response to sudden changes in the solar wind, *Geophys. Res. Lett.*, ***15***, 253-256, 1988.

Gazey, N.G.J., M. Lockwood, P.N. Smith, S. Coles, R.J. Bunting, M. Lester, A.D. Aylward, T.Y. Yeoman and H. Lühr, The development of substorm cross-tail current disruption as seen from the ground, *J. Geophys. Res.*, in press, 1995.

Glaßmeier, K-H., Travelling magnetospheric convection twin-vortices: observations and theory, *Ann. Geophys.*, ***10***, 547-565, 1992.

Glaßmeier, K.-H., M. Hoenisch and J. Untied, Ground-based and satellite observations of travelling magnetospheric convection twin vortices, *J. Geophys. Res., 94,* 2520-2528, 1989.

Grande, M., C. H. Perry, D. S.Hall, B. Wilken, S. Livi, F. Søraas, and J. F. Fennel, Composition signatures of substorm injections, in *Proceedings of the International Conference on Substorms (ICS-1)*, Kiruna, Sweden, March 1992, *ESA SP-335*, pp. 111-116, 1992

Grande, M., C. H. Perry, H. J. Opgenoorth, and N. W. Watkins, Multiple injection substorms, source material and small scale morphology, in *Proceedings of the International Conference on Substorms (ICS-2)*, Fairbanks, Alaska, March 1994, in press, 1994

Greenwald, R.A., K.B. Baker, J.M. Ruohoniemi, J.R. Dudeney, N. Pinnock, N. Mattin, J.M. Leonard, and R.P. Lepping, Simultaneous conjugate observations of dynamic variations in high-latitude dayside convection due to changes in IMF B_y, *J. Geophys. Res.*, ***95***, 8057-8072, 1990.

Gustafsson, G., N.E. Papitashvili, and V.O. Papitashvili, A revised corrected geomagnetic coordinate system for Epochs 1985 and 1990, *J. Atmos. Terr. Phys.*, *54*, 1609-1631, 1992.

Hanuise, C., C. Senior, J-C.Cerisier, J.-P. Villain, R.A.Greenwald, J.M. Ruohoniemi, and K.B. Baker, Instantaneous mapping of high-latitude convection with coherent HF radars, *J. Geophys. Res.*, ***98***, 17387-17400 , 1993.

Heelis, R. A., and W.R. Coley, Global and local Joule heating effects seen by DE-2, *J. Geophys. Res., 93,* 7551-7557.

Heikkila, W.J., T.S. Jorgensen, L.J. Lanzerotti and C.J. Maclennan, A transient auroral event on the dayside, *J. Geophys. Res.*, 94, 15,291-15,305, 1989.

Hesse, M., and J. Birn, Magnetosphere-ionosphere coupling during plasmoid evolution: first results, *J. Geophys. Res.*, ***96***, 11,513-11,522, 1991

Hones, E. W. Jr., J. D. Craven, L. A. Frank, D. S. Evans and P. T. Newell, The horse-collar aurora: a frequent pattern of the aurora in quiet times, *Geophys. Res. Lett., 16*, 37-40, 1989.

Jacobsen, B., P.E. Sandholt, B.Lybekk, and A. Egeland, Transient auroral events near midday: relationship with solar wind/magnetosheath plasma and magnetic field conditions, *J. Geophys. Res.*, ***96***, 1327-1336, 1991.

Kan, J.R., A global magnetosphere-ionosphere coupling model of substorms, *J. Geophys. Res.*, ***98***, 17263-17276, 1993.

Kamide Y., S.-I. Akasofu, S.E. Deforest, J. L. Kisabeth, Weak and intense substorms, *Planet. Space Sci., 23*, 579-587, 1975

Kamide, Y., P.D. Perreault, S.-I. Akasofu, and D. Winningham, Dependence of substorm occurrence probability on the interplanetary magnetic field and on the size of the auroral oval, *J. Geophys. Res.*, 82, 5521-5528, 1977

Kaufmann,R.L., Substorm currents: Growth phase and onset, *J. Geophys. Res., 92,* 7471-7486,

1987.

Kennel, C., The Kiruna Conjecture: The strong version, in *Proceedings of the International Conference on Substorms (ICS-1)*, Kiruna, Sweden, March 1992, *ESA SP-335*, pp. 599-601, 1992

Kirkwood, S., L. Eliasson, H. J. Opgenoorth, and A. Pellinen-Wannberg, A study of auroral electron acceleration using the EISCAT radar and the Viking satellite, *Adv. Space Res., 9*, 49-52, 1989.

Kirkwood S. and L. Eliasson, Energetic particle precipitation in the substorm growth phase measured by Eiscat and Viking, *J. Geophys. Res.*, 95, 6025-6037, 1990.

Kirkwood, S., H. J. Opgenoorth, and J. S. Murphree, Ionospheric conductivities, electric fields and currents associated with auroral substorms measured by the EISCAT radar, *Planet. Space Sci., 36*, 1359-1380, 1988.

Kivelson, M.G., and D.J. Southwood, Ionospheric travelling vortex generation by solar wind buffeting of the magnetosphere, *J. Geophys. Res., **96**,* 1661-1667, 1991.

Knipp, D., B.A. Emery, A.D. Richmond, N.U. Crooker, M.R. Hairston, J.A. Cumnock, W.F. Denig, F.J. Rich, O. del la Beaujardiere, J.M. Ruohoniemi, A.S. Rodger, G. Crowley, B.-H. Ahn, D.S. Evans, T.J. Fuller-Rowell, E. Friis-Christiansen, M. Lockwood, H. Kroehl, C. McClennan, A, McEwin, R.J. Pellinen, R.J. Morris, G.B. Burns, V. Papitashvili, A.Zaitzev, O. Troshichev, N. Sato, P. Sutcliffe, L. Tomlinson, Ionospheric convection response to strong, slow variations in a northward interplanetary magnetic field: A case study for January 14, 1988, *J. Geophys. Res.*, *98*, 19,273-19,292, 1993.

Koskinen, H. E. J., T. I. Pulkkinen, R. J. Pellinen, T.Bösinger, D. N. Baker, and R.E. Lopez, Characteristics of Pseudobreakups, in *Proceedings of the International Conference on Substorms (ICS-1)*, Kiruna, Sweden, March 1992, *ESA SP-335*, pp. 111-116, 1992

Lockwood, M., Ground-Based and Satellite Observations of the Cusp: Evidence for Pulsed Magnetopause Reconnection, in *"Physics of the magnetopause"*, ed. B.U.O. Sonnerup, Proc. Chapman Conf. on the Magnetopause, American Geophysical Union Monograph, in press, 1995a.

Lockwood, M., Large-scale fields and flows in the magnetosphere-ionosphere system, *Surveys in Geophysics*, in press, 1995b.

Lockwood, M., and S.W. Cowley, Ionospheric convection and the substorm cycle, Substorms 1, *Proceedings of the First International Conference on Substorms, (ICS-1)*, Kiruna, Sweden, March 1992, *ESA-SP-335*, pp 99-110, 1992.

Lockwood, M., and H.J. Opgenoorth, Opportunities for magnetospheric research using EISCAT/ESR and CLUSTER, *J. Geoelect. Geomag.*, submitted, 1995.

Lockwood, M., and M.F. Smith, Low- and mid-altitude cusp particle signatures for general magnetopause reconnection rate variations: I - Theory, *J. Geophys. Res., 99*, 8531-8555, 1994.

Lockwood, M., M.O. Chandler, J.L Horwitz, J.H. Waite, Jr., T.E. Moore, and C.R. Chappell, The cleft ion fountain, *J. geophys. Res., 90,* 9736-9748, 1985.

Lockwood, M., P.E. Sandholt, S.W.H. Cowley, and T. Oguti, Interplanetary magnetic field control of dayside auroral activity and the transfer of momentum across the dayside magnetopause, *Planet. Space Sci., 37,* 1347-1365, 1989.

Lockwood M., W.F. Denig, A.D. Farmer, V.N. Davda, S.W. Cowley, and H. Lühr, Ionospheric signatures of pulsed reconnection at the earth's magnetopause, *Nature, **361**,* 424-427, 1993a

Lockwood, M., H.C. Carlson and P.E. Sandholt, The implications of the altitude of transient 630 nm dayside auroral emissions, *J. geophys. Res., 98,* 15571-15587, 1993b.

Lockwood, M., T.G. Onsager, C.J. Davis, M.F. Smith and W.F Denig, The characteristics of the magnetopause reconnection X-line deduced from low-altitude satellite observations of cusp ions, *Geophys. Res. Lett. 21*, 2757-2760, 1994.

Lopez, R.E., H.E.J. Koskinen, T.I. Pulkkinen, T. Bosinger, R.W. McEntire, and T.A. Potemra, Simultaneous observation of the poleward expansion of substorm electrojet activity and the tailward expansion of current sheet disruption in the near-earth magnetotail, *J. Geophys. Res., **98**,* 9285-9295, 1993.

Lui, A. T. Y., S.-I. Akasofu, E. W.Hones, S. J. Bame, and C. E. McIlwain, Observations of the Plasma sheet during a contracted oval substorm in a prolonged quiet period, *J. Geophys. Res., 81,* 1415-1419, 1976.

Lui, A. T. Y., R. E. Lopez, B. J. Anderson, K. Takahashi, L. J. Zanetti, R. W. McEntire, T. A. Potemra, D. M. Klumpar, E. M. Greene, and R. Strangeway, Current disruptions in the near-Earth neutral sheet region, *J. Geophys. Res., 97,* 1461-1480, 1992

Lühr, M. Lockwood, P.A. Sandholt, T.L. Hansen and T. Moretto, Multi-instrument ground-based observations of a Travelling Convection Vortex event, *Annales Geophys.*, submitted, 1995

Lysak, R.L., and D.-H. Lee, Response of the dipole magnetosphere to pressure pulses, *Geophys. Res. Lett., **19,*** 937-940, 1992.

McPherron R.L., V. Angelopoulos, D.N. Baker, and E.W. Hones, Jr., Is there a near-earth neutral line? *Adv. Space Res., **13,*** (4)173-(4)186, 1993.

Murphree, J. S., and L. L. Cogger, Observed connections between apparent polar cap features and the instantaneous diffuse auroral oval, *Planet. Space Sci., 29*, 1143, 1981.

Murphree, J.S., R.D. Elphinstone, L.L. Cogger and D.D. Wallis, Short-term dynamics of the high-latitude auroral distribution, *J. Geophys. Res., 94,* 6969-6974, 1989.

Moldwin, M.B., and W.J. Hughes, On the formation and evolution of plasmoids: A survey of ISEE 3 geotail data, *J. Geophys. Res., **97,*** 19,259-19,282, 1992

Morelli, J.P., R.J. Bunting, S.W.H. Cowley, C.J. Farrugia, M.P. Freeman, E. Friis-Christensen, G.O.L. Jones, M. Lester, R.V. Lewis, H. Lühr, D. Orr, M. Pinnock, G.D. Reeves, P.J.S. Williams, and T.K.Yeoman, Plasma flow bursts in the nightside auroral zone ionosphere and their relation to geomagnetic activity, *Adv. Space Res., **13,*** (4)135-(4)138, 1993.

Newell, P.T. and C.-I. Meng, Mapping the dayside ionosphere to the magnetosphere according to particle precipitation characteristics, *Geophys. Res. Lett., **19,*** 609-612, 1992.

Newell, P.T.,C.-I. Meng, D.G. Sibeck and R. Lepping, Some low-altitude cusp dependencies on the interplanetary magnetic field, *J. Geophys. Res., 94,* 8921-8927, 1989

Newell, P.T. W.J. Burke, E.R. Sanchez, Ching-I. Meng, M.E. Greenspan, and C.R. Clauer, The low-latitude boundary and the boundary plasma sheet at low altitude: prenoon precipitation regions and convection reversal boundaries, *J. Geophys. Res., **96,*** 21,013-21,023, 1991.

Norberg O., M. Yamauchi, L. Eliasson and R. Lundin, Freja observations of multiple injection events in the cusp, *Geophys. Res. Lett., 21,* 1919-1922, 1994.

Onsager T.G., C.A. Kletzing, J.B. Austin, and H. MacKiernan, Model of magnetosheath plasma in the magnetosphere: Cusp and mantle particles at low-altitudes, *Geophys. Res. Lett., **20,*** 479-482, 1993.

Onsager, T.G., et al., Low-altitude observations and modelling of quasi-steady reconnection, *J.Geophys.Res.*, in press, 1994.

Opgenoorth, H.J., Coordination of ground-based observations with Cluster, in *Cluster: mission, payload and supporting activities, ESA-SP-1159*, pp. 301-305, 1993.

Opgenoorth, H. J., B.Bromage, D. Fontaine, C. La Hoz, A. Huuskonen,H. Kohl, U. P. Løvhaug, G. Wannberg, G. Gustavsson, J. S. Murphree, L. Eliasson, G. Marklund, T. A. Potemra, S. Kirkwood, E. Nielsen, and J.-E. Wahlund, Coordinated observations with EISCAT and the Viking satellite: The decay of a westward travelling surge, *Ann. Geophys.*, 7, 479-500, 1989.

Opgenoorth, H. J., M. A. L. Persson, T. I. Pulkkinen, and R. J. Pellinen, The recovery phase of magnetospheric substorms and its association with morning -sector aurora, *J. Geophys. Res., 99,* 4115-4129, 1994

Owen, C.J., and J.A. Slavin, Energetic ion events associated with travelling compression regions, in *Proceedings of the First International Conference on Substorms, (ICS-1)*, Kiruna,

Swede, March 1992, *ESA-SP-335*, pp. 365-370, 1992.

Pellinen, R. J., H. J. Opgenoorth, and T. I. Pulkkinen, Substorm recovery phase: relationship to next activation, *Proceedings of the International Conference on Substorms (ICS-1)*, Kiruna, Sweden, March 1992, *ESA SP-335*, pp. 469-475, 1992

Pellinen, R. J., H. E. J. Koskinen, T. I. Pulkinen, J. S. Murphree, G. Rostoker, and H. J. Opgenoorth, Satellite and ground-based observations of a fading transpolar arc, *J. Geophys. Res., 95,* 5817-5824, 1990

Persson, M. A. L., H. J. Opgenoorth, T. I. Pulkkinen, A. I. Ericsson, P. O. Dovner, G. D. Reeves, R. D. Belian, M. Andre, L. G. Blomberg, R. E. Erlandson, M. H. Boehm, A. T. Aikio, and I. Häggström, Near-Earth substorm onset: A coordinated study, *Geophys. Res. Lett., 21*, 1875-1878, 1994a

Persson, M. A. L., A. Aikio, and H. J. Opgenoorth, Satellite-groundbased coordination: Late growth phase and early expansion phase of a substorm, in *Proceedings of the International Conference on Substorms (ICS-2)*, Fairbanks, Alaska, March 1994}, in press, 1994b

Pinnock M., A.S. Rodger, J.R. Dudeney, K.B. Baker, P.T. Newell, R.A. Greenwald, and M.E. Greenspan, Observations of an enhanced convection channel in the cusp ionosphere, *J. Geophys. Res.,* ***98,*** 3767-3776, 1993.

Potemra, T.A., R.E. Erlandson, L.J. Zanetti, R.L. Arnold, J. Woch, and E. Friis-Christensen, The dynamic cusp, *J. Geophys. Res., 97*, 2835-2844, 1992.

Pulkkinen, T. I., D. N. Baker, R. J. Pellinen, J. Buechner, H. E. J. Koskinen, R. E. Lopez, R. L. Dyson, and L. A. Frank, Particle scattering and current sheet stability in the Geomagnetic tail during the substorm growth phase, *J. Geophys. Res., 97*, 19283-19297, 1992.

Richmond, A.D., Assimilative mapping of ionospheric electrodynamics, *Adv. Space Res.,* ***12,*** (6)59-(6)68, 1992.

Rodger, A.S., M. Pinnock, J.R. Dudeney, K.B. Baker and R.A. Greenwald, A new mechanism for polar patch formation, *J. Geophys. Res., 99*, 6425-6436, 1994a.

Rodger, A.S., M. Pinnock, J.R. Dudeney, J. Waterman, O. de la Beaujardiere, and K.B. Baker, Simultaneous two-hemisphere observations of the presence of polar patches in the night ionosphere, *Ann. Geophys, 12,* 642-648, 1994b.

Rodriguez-Canabal, J., M. Warhaut, R. Schmidt and M. Bello-Mora, The Cluster orbit and mission scenario, in *Cluster: mission, payload and supporting activities, ESA-SP-1159*, pp. 259-278, 1993.

Sanchez, E.R., G.L. Siscoe, and C.-I. Meng, Inductive attenuation of the transpolar voltage, *Geophys. Res. Lett.,* ***18,*** 1173-1176, 1991.

Sandholt, P.E., A. Egeland, J.A. Holtet, B. Lybekk, K.Svenes, and S. Asheim, S., Large- and small-scale dynamics of the polar cusp, *J. Geophys. Res., 90,* 4407-4414, 1985.

Sandholt, P. E., M. Lockwood, T. Oguti, S. W. H. Cowley, K. S. C. Freeman, B. Lybekk, A. Egeland, and D. M. Willis, Midday auroral breakup events and related energy and momentum transfer from the magnetosheath, *J. Geophys. Res., 95,* 1039-1060, 1990.

Schmidt, R., and M.L. Goldstein, Cluster - a fleet of four spacecraft to study plasma structures in three dimensions, in *The Cluster Mission, ESA-SP-1103*, pp. 7-13, 1988.

Sergeev, V.A., R.C. Elphic, F.S. Mozer, A. Saint-Marc and J.A. Sauvard, A two-satellite study of nightside flux transfer events in the plasma sheet, *Planet. Space Sci.,* ***11,*** 1551-1572, 1992.

Slavin, J.A., M.F. Smith, E.L. Mazur, D.N. Baker, T. Iyemori, H.J. Singer, and E.W. Greenstadt, ISEE 3 plasmoid and TCR observations during an extended interval of substorm activity, *Geophys. Res. Lett.,* ***19,*** 825-828, 1992.

Smith, M.F. and D.J. Rodgers, Ion distributions at the dayside magnetopause, *J. Geophys. Res.,* ***96,*** 11,617-11,624, 1991.

Untiedt, J., R. Pellinen, F. Küppers, H. J. Opgenoorth, W. D. Pelster, W. Baumjohann, H. Ranta, J. Kangas, P. Chechowsky, and W. Heikkila, Observations of the initial development of an auroral and magnetic substorm at magnetic midnight, *J. Geophys., 45*, 41-65, 1978.

Wahlund, J.-E., and H. J. Opgenoorth, EISCAT observations of strong ion outflows from the F-region ionosphere during auroral activity: Preliminary results, *Geophys. Res. Lett., 16,* 727-730, 1989.

Wahlund, J. E., H. J. Opgenoorth, I. Häggström, K. J. Winser, G. O. L. Jones, EISCAT observations of topside ionospheric ion outflows during auroral activity: Revisited, *J. Geophys. Res., 97*, 3019-3037, 1992.

Weiss, L. A., P. H. Reiff, J. J. Moses, R. A. Heelis, and B. D. Moore, Energy dissipation in substorms, in *Proceedings of the International Conference on Substorms (ICS-1)*, Kiruna, Sweden, March 1992, *ESA SP-335*, pp. 309-317, 1992

Weiss, L.A., P.H. Reiff, H.C. Carlson, E.J. Weber and M. Lockwood, Flow-aligned jets in the magnetospheric cusp: results from the GEM pilot programme,
J. Geophys. Res., in press, 1995.

Yeoman, T. K, H. Lühr, R. W. H. Friedel, S. Coles, M. Grande, C. H. Perry, M. Lester, P.N. Smith, H.J. Singer, and D. Orr, CRRES/Ground-Based multi-instrument observations of an interval of substorm activity, *Ann. Geophys.*, in press, 1994

Table 1. GROUND BASED - CLUSTER EXPERIMENTS

#		Ground-based site location	Cluster location	Scientific Objectives (see Table II)
1	VHP	midnight AO and PC	tail NS	a,b,c,d,e,f,g,h,i,j,A,l,m,r,s,t,H,k,n,v,B,w,J
2	HP	midnight AO and PC	lobe	c,f,g,h,A,m,G,r,s,t,J,v,C,w
2*		midnight AO and PC	lobe	c,f,g,h,G,r,s,t,J,v,C,D,w
3		midnight AO and PC	interior cusp	o,r,u
4		midnight AO and PC	dayside RC	p,q,j,E,F
5	VHP	cusp/cleft	interior cusp	α,Ω,π,β,γ,δ,ε,ζ,η,θ,Λ,σ,λ,τ,ξ,Δ,μ,A,J,G,Θ,Σ
5*	HP	cusp/cleft	interior cusp	α,Ω,π,β,γ,δ,ζ,Λ,A,D,Θ,Δ,μ,J
6	HP	cusp/cleft	lobe	r,α,Ω,π,ξ,τ
6*		cusp/cleft	lobe	r,α,Ω,π,ξ,
7		cusp/cleft	tail NS	o,r,l,τ
8	HP	dawn AO and PC	interior cusp	μ,ξ,Λ,θ,r,G,s
8*		dawn AO and PC	interior cusp	r,s
9		dawn AO and PC	lobe	r,s,t,G,c,C,f,v,B,k,w
9*		dawn AO and PC	lobe	r,s,t,c,f,k,v,B,w
10	HP	dawn AO and PC	tail NS	r,s,t,k,w
11		dawn AO and PC	dayside RC	q,p,s,t,E,F,w
12	HP	dusk AO and PC	interior cusp	Δ,μ,ξ,Λ,θ,r,s
12*		dusk AO and PC	interior cusp	r,s
13		dusk AO and PC	lobe	r,s,t,G,n,v,B,w
13*		dusk AO and PC	lobe	r,s,t,n,v,B,w
14	HP	dusk AO and PC	tail NS	r,s,t,c,f,n,v,B
15		dusk AO and PC	dayside RC	q,p,s,t,E,F,χ,j
16		midnight AO and PC	SW	u,I
17		midnight AO and PC	exterior cusp	u,o,J,r
17*		midnight AO and PC	exterior cusp	u,o,J,r
18		midnight AO and PC	near-Earth lobe	c,f,G,C,J
18*		midnight AO and PC	near-Earth lobe	c,f,G,C,J
19	HP	midnight AO and PC	midnight AO	H,i,j,A,B,r,v,k,n,e
19*		midnight AO and PC	midnight AO	B,r,v,k,n,e
20		midnight AO and PC	nightside RC	p,q,E
21	HP	cusp/cleft	SW	δ,ε,ξ,Θ,Λ ,α,Ω,π,Σ,Γ,ψ
22	VHP	cusp/cleft	exterior cusp	α,Ω,π,β,γ,δ,ε,Θ,η,θ,Λ,A,σ,μ,τ,ξ,ϕ,ψ,Γ,Δ,Ξ,Σ
22*	HP	cusp/cleft	exterior cusp	α,Ω,π,β,γ,δ,η,Λ,A,σ,μ,τ,ξ,ψ,Γ,Δ,D,Ξ,Σ
23	HP	cusp/cleft	near-Earth lobe	r,τ,ξ,Δ,G,C,J,A
23*		cusp/cleft	near-Earth lobe	r,τ,ξ,Δ,G,C,J,D
24		cusp/cleft	midnight AO	o,J,G,r,v
24*		cusp/cleft	midnight AO	o,J,G,r,v
25		cusp/cleft	midnight RC	o,p,q,τ
26	HP	dawn AO and PC	SW	s,r,t,u,I,J,k,θ,Λ,λ,μ,ξ,ψ,Γ,G
27	VHP	dawn AO and PC	exterior cusp	s,r,u,I,J,k,α,Ω,π,β,γ,δ,θ,Λ,σ,λ,μ,ξ,ϕ,ψ,Γ,G,Σ
27*	HP	dawn AO and PC	exterior cusp	s,r,u,I,J,k,α,Ω,π,β,γ,δ,θ,Λ,λ,μ,ξ,ϕ,ψ,Γ,D,G,Σ

(Table 1, continued)

28	HP	dawn AO and PC	near-Earth lobe	s,t,r,B,τ,f,c,G,J,C,w
28*		dawn AO and PC	near-Earth lobe	s,t,r,B,f,c,G,J,C,w
29		dawn AO and PC	midnight AO	s,t,r,B,e,k,w
29*		dawn AO and PC	midnight AO	s,t,r,B,e,k,w
30		dawn AO and PC	midnight RC	p,q,s,t,r,E
31		dusk AO and PC	SW	s,r,t,u,I,J,k,θ,Λ,λ,μ,ξ,ψ,Γ,χ,G
32	VHP	dusk AO and PC	exterior cusp	s,r,u,I,J,α,Ω,π,β,γ,δ,θ,Λ,σ,λ,μ,ξ,ϕ,ψ,Γ,χ,G,Σ,Ξ
32*	HP	dusk AO and PC	exterior cusp	s,r,u,I,J,α,Ω,π,β,γ,δ,θ,Λ,λ,ξ,ϕ,ψ,Γ,D,χ,G,Σ,Ξ
33	HP	dusk AO and PC	near-Earth lobe	s,t,r,B,χ,f,c,C,G,J,w
33*		dusk AO and PC	near-Earth lobe	s,t,r,B,χ,f,c,C,G,J,w
34		dusk AO and PC	midnight AO	s,t,r,B,e,n,χ,o,w
34*		dusk AO and PC	midnight AO	s,t,r,B,e,n,χ,o,w
35		dusk AO and PC	midnight RC	p,q,s,t,r,χ,E,n,w
36		midnight AO and PC	dawn RC	p,q,E,k,w
37		midnight AO and PC	dawn AO	r,s,t,B,k,v ,w
37*		midnight AO and PC	dawn AO	r,s,t,B,k,v,w
38	HP	midnight AO and PC	near-Earth lobe	s,t,r,f,c,B,C,J,G,v,w
38*		midnight AO and PC	near-Earth lobe	s,t,r,f,c,B,C,J,G,v,w
39		midnight AO and PC	dusk MP	I,u,o
39*		midnight AO and PC	dusk MP	I,u,o
40		cusp/cleft	dawn RC	r,p,q,E
41	HP	cusp/cleft	dawn AO	r,B,α,Ω,π,β,δ,θ,Λ,A,σ,λ,μ,ξ,Δ
41*		cusp/cleft	dawn AO	r,B,α,Ω,π,β,δ,θ,Λ,A,σ,λ,μ,ξ,Δ
42	HP	cusp/cleft	near-Earth lobe	r,ξ,τ,G,J,C,α,Ω,π
42*	HP	cusp/cleft	near-Earth lobe	r,ξ,τ,G,J,C,α,Ω,π,D
43	VHP	cusp/cleft	dusk MP	A,α,Ω,π,Ξ,β,γ,δ,θ,Λ,σ,λ,ξ,ϕ,ψ,Γ,Δ,Θ,ε,η
43*	VHP	cusp/cleft	dusk MP	A,α,Ω,π,Ξ,β,γ,δ,θ,Λ,σ,λ,ξ,ϕ,ψ,Γ,Δ,Θ,D
44		dawn AO and PC	dawn RC	p,q,E,s,t,r,A,m,k,v,B
45	VHP	dawn AO and PC	dawn AO	H,r,s,t,k,θ,λ,Λ,σ,α,Ω,π,A,m,v,B,w
45*		dawn AO and PC	dawn AO	r,s,t,k,θ,λ,Λ,σ,α,Ω,π,D,A,m,v,B,w
46	HP	dawn AO and PC	near-Earth lobe	r,s,t,k,c,f,J,G,B,C,m,v,μ,ξ
46*		dawn AO and PC	near-Earth lobe	r,s,t,k,c,f,J,G,B,C,m,v,μ,ξ
47		dawn AO and PC	dusk MP	r,s,t,Γ,σ,I,ϕ,ψ,u,Λ
47*		dawn AO and PC	dusk MP	r,s,t,Γ,σ,I,ϕ,ψ,u,Λ
48		dusk AO and PC	dawn RC	p,q,r,s,t,E
49		dusk AO and PC	dawn AO	r,s,t,Λ,v,B
49*		dusk AO and PC	dawn AO	r,s,t,Λ,v,B
50	HP	dusk AO and PC	near-Earth lobe	r,s,t,n,c,f,J,G,B,C,χ,m,v,μ,ξ
50*		dusk AO and PC	near-Earth lobe	r,s,t,n,c,f,J,G,B,C,χ,m,v,μ,ξ
51	VHP	dusk AO and PC	dusk MP	r,s,t,B,χ,θ,λ,Λ,σ,ψ,Γ,ϕ,n,A,Ξ
51*	HP	dusk AO and PC	dusk MP	r,s,t,θ,λ,Λ,σ,ψ,Γ,ϕ,n,D,Ξ
52		midnight AO and PC	dawn MP	I,u
52*		midnight AO and PC	dawn MP	I,u
53	HP	midnight AO and PC	near-Earth lobe	s,t,r,f,c,B,C,J,G,g,i,v,B,w
53*		midnight AO and PC	near-Earth lobe	s,t,r,f,c,B,C,J,G,g,i,v,B,w
54		midnight AO and PC	dusk AO	χ,e,n,m,t,w

(Table 1, continued)

54*		midnight AO and PC	dusk AO	χ,e,n,m,t,w
55		midnight AO and PC	dusk RC	p,q,E,F,e,g,i,j,l,m,B,v
56	VHP	cusp/cleft	dawn MP	A,α,Ω,π,Ξ,β,γ,δ,θ,Λ,σ,λ,ξ,ϕ,ψ,Γ,Δ,Θ,ε,η
56*	VHP	cusp/cleft	dawn MP	A,α,Ω,π,Ξ,β,γ,δ,θ,Λ,σ,λ,ξ,ϕ,ψ,Γ,Δ,Θ,D,ε,η
57	HP	cusp/cleft	near-Earth lobe	r,ξ,τ,G,J,C,α,Ω,π,A
57*	HP	cusp/cleft	near-Earth lobe	r,ξ,τ,G,J,C,α,Ω,π,D
58	HP	cusp/cleft	dusk AO	r,s,n,B,α,Ω,π,β,ζ,θ,Λ,A,σ,λ,μ,ξ,Δ,χ
58*		cusp/cleft	dusk AO	r,s,n,B,α,Ω,π,β,ζ,θ,Λ,A,σ,λ,μ,ξ,Δ,χ
59		cusp/cleft	dusk RC	p,q,E,F,τ,r
60	VHP	dawn AO and PC	dawn MP	r,s,t,B,θ,λ,Λ,σ,ψ,Γ,ϕ,k,A,Ξ
60*	HP	dawn AO and PC	dawn MP	r,s,t,θ,λ,Λ,σ,ψ,Γ,ϕ,k,D,Ξ
61	HP	dawn AO and PC	near-Earth lobe	r,s,t,k,c,f,J,G,B,C,χ,m,v,μ,ξ,w
61*		dawn AO and PC	near-Earth lobe	r,s,t,k,c,f,J,G,B,C,χ,m,v,μ,ξ,w
62		dawn AO and PC	dusk AO	r,s,t,v,B,Λ,w
62*		dawn AO and PC	dusk AO	r,s,t,v,B,Λ,w
63		dawn AO and PC	dusk RC	p,q,r,s,t,E,F,w
64		dusk AO and PC	dawn MP	r,s,t,Γ,σ,I,ϕ,ψ,u,Λ,χ
64*		dusk AO and PC	dawn MP	r,s,t,Γ,σ,I,ϕ,ψ,u,Λ,χ
65	HP	dusk AO and PC	near-Earth lobe	r,s,t,n,c,f,J,G,B,C,m,v,μ,ξ,w
65*		dusk AO and PC	near-Earth lobe	r,s,t,n,c,f,J,G,B,C,m,v,μ,ξ,w
66	VHP	dusk AO and PC	dusk AO	H,r,s,t,n,θ,λ,Λ,σ,A,v,B,m,χ,w
66*		dusk AO and PC	dusk AO	r,s,t,n,θ,λ,Λ,σ,D,v,B,m,χ,w
67		dusk AO and PC	dusk RC	p,q,E,F,s,t,r,A,m,n,v,B,χ,w

abbreviations: AO = auroral oval; HP = high priority; MP = magnetopause; NS = neutral sheet; PC = polar cap; RC = ring current; SW = Solar Wind; VHP = very high priority
*Configuration numbers labelled * have satellites in opposite hemisphere to ground-based site*

Table 2. SCIENTIFIC OBJECTIVES

Tail phenomena and substorms

a. Location of substorm onset
b. Location of near-Earth neutral line (NENL)
c. Onset time of substorm-enhanced tail reconnection
d. Mechanisms for cross-tail current disruption (CD)
e. Development of CD and evolution into NENL
f. Energy release from tail lobe
g. Pseudobreakups
h. Structure, evolution and pinch-off time of plasmoids
i. Southward-drifting arcs
j. Nightside ionospheric outflows and tail composition
k. Omega bands
l. Plasma sheet (PS) thinning
m. Field aligned currents and precipitation as a function of substorm phase
n. Westward travelling surge
o. Connection of dayside and nightside auroral intensifications
p. Asymmetric ring current
q. Energetic particle injection
r. Substorm growth phase
s. Polar cap expansion and contraction
t. Convection during substorms
u. IMF and SW triggers of substorms
v. Recovery phase
w. Activations along a contracted auroral oval

General magnetospheric topology, morphology and dynamics

A. Mapping electric and magnetic fields
B. Double auroral oval and open/closed boundary
C. Lobe field topology (bifurcation and asymmetries)
D. Conjugacy and interhemispheric symmetries and asymmetries
E. Time-dependency of RC drift shells and splitting
F. Detached plasmasphere regions and ionospheric plasma in the dayside magnetosphere
G. Transpolar and other polar cap arcs
H. Auroral acceleration
I. IMF control of convection
J. NBz convection

Magnetopause and boundary-layers

α. Effects of magnetopause reconnection
β. Location of dayside X-line
γ. Conditions at dayside X-line
δ. Causes of magnetopause reconnection rate variations

(Table 2, continued)

ε. Ion transmission factors across magnetopause
ζ. Cusp ions steps and temporal and spatial variations
η. Maintenance of cusp quasi-neutrality
θ. Open and closed low-latitude boundary layers (LLBL)
Λ. Origin, propagation and lifetime of travelling convection vortices (TCVs)
σ. Field-aligned currents and precipitation in TVCs
λ. Voltage and thickness of LLBL
μ. Local time extent of dayside transients
τ. Origin of cleft ion fountain and effects on lobe and PS composition
ξ. Voltage contribution of reconnection pulses
φ. Magnetopause oscillations and surface waves
χ. Mid-afternoon auroral bright spot
ψ. IMF control of dayside ionospheric transients, TCVs and magnetopause flux transfer events (FTEs)
Γ. SW pressure pulses as a cause of TCVs, magnetopause FTEs and reconnection pulses
Δ. Spatial distribution and origins of dayside field aligned current
Θ. Ion acceleration at the magnetopause
Ξ. Motion of newly-reconnected field lines
Σ. Origin of polar cap patches
Ω. Origin of dayside ionospheric transients
π. Ionospheric signatures of magnetopause FTEs

Table 3. THE REPETITION OF A CONFIGURATION FOR AN ORBIT PERIOD OF 57 HOURS

Orbit Number	Day Number	UT (hrs)	MLT difference of GB station from satellite, δL (hrs)	Deviation of satellite MLT from ideal, δMLT (hrs)
1	1	9	0	0
2	3	18	9	0.156
3	6	3	-6	0.312
4	8	12	3	0.468
5	10	21	12	0.642
6	13	6	-3	0.780
7	15	15	6	0.936
8	18	0	-9	1.092
9	20	9	0	1.248

Table 4. SAMPLE OUTPUT OF PREDICTION PROCEDURE (configuration 1 only)

Cluster Orbit Predictions

****

Station

EISCAT Tromso : Latitude 69.6 : Longitude 19.2

Configurations

1

Event	DD/MM/YYYY	UT	Cluster MLT	Ground MLT	GB_MLT - IMLT	Prediction status	Config	Priority
NS_001_N	21/12/1995	16.38	23.2	18.67	-4.5	T	1	VHP
AP_001	21/12/1995	17.16	23.2	19.33	-3.9	T	1	VHP
AP_002	24/12/1995	2.24	22.8	4.25	5.4	T	1	VHP
NS_002_S	24/12/1995	6.29	23.0	8.74	9.7	T	1	VHP
NS_003_N	26/12/1995	11.21	22.9	13.70	-9.2	T	1	VHP
AP_003	26/12/1995	11.24	22.9	13.74	-9.2	T	1	VHP
AP_004	28/12/1995	20.16	22.6	22.06	-0.5	T	1	VHP
NS_004_S	29/12/1995	1.96	22.4	3.89	5.5	T	1	VHP
AP_005	31/12/1995	5.24	22.4	7.51	9.1	T	1	VHP
NS_006_N	2/ 1/1996	12.79	2.4	15.32	-7.1	T	1	VHP
AP_006	2/ 1/1996	14.25	22.4	16.74	-5.7	T	1	VHP
AP_007	4/ 1/1996	23.33	22.0	1.10	3.1	T	1	VHP
NS_007_S	5/ 1/1996	4.21	22.0	6.32	8.3	T	1	VHP
AP_009	9/ 1/1996	17.33	21.8	19.35	-2.4	T	1	VHP
NS_009_S	9/ 1/1996	23.54	21.5	1.28	3.8	T	1	VHP
AP_010	12/ 1/1996	2.33	21.4	4.20	6.8	T	1	VHP
NS_011_N	14/ 1/1996	10.13	21.5	12.37	-9.1	T	1	VHP
AP_011	14/ 1/1996	11.33	21.6	13.64	-8.0	T	1	VHP
AP_012	16/ 1/1996	20.33	21.3	22.13	0.8	T	1	VHP
NS_012_S	17/ 1/1996	3.04	21.0	4.95	8.0	T	1	VHP
NS_014_N	21/ 1/1996	12.79	21.1	15.12	-6.0	T	1	VHP
AP_014	21/ 1/1996	14.41	21.0	16.71	-4.3	T	1	VHP
NS_014_S	21/ 1/1996	21.96	20.7	23.70	3.0	T	1	VHP
NS_132_N	27/10/1996	19.54	2.9	21.90	5.0	T	1	VHP
AP_132	27/10/1996	21.42	2.8	23.73	3.1	T	1	VHP
AP_134	1/11/1996	15.50	2.6	18.03	8.6	T	1	VHP
NS_134_S	1/11/1996	16.04	2.6	18.53	8.1	T	1	VHP
NS_135_N	3/11/1996	21.46	2.4	23.74	2.7	T	1	VHP
AP_135	4/11/1996	0.50	2.4	2.75	0.3	T	1	VHP
AP_136	6/11/1996	9.50	2.4	12.06	9.7	T	1	VHP
NS_137_N	8/11/1996	16.87	2.1	19.30	6.8	T	1	VHP
AP_137	8/11/1996	18.50	2.1	20.84	5.3	T	1	VHP
AP_138	11/11/1996	3.58	2.1	6.01	3.9	T	1	VHP
NS_138_S	11/11/1996	8.46	2.2	11.05	8.8	T	1	VHP

(Table 4, continued)

NS_139_S	13/11/1996	13.46	1.9	16.18	9.7	T	1	VHP
NS_140_N	15/11/1996	18.21	1.6	20.53	5.1	T	1	VHP
AP_140	15/11/1996	21.67	1.5	23.88	1.6	T	1	VHP
AP_141	18/11/1996	6.67	1.7	9.31	7.6	T	1	VHP
NS_142_N	20/11/1996	14.37	1.4	17.05	8.3	T	1	VHP
AP_142	20/11/1996	15.67	1.4	18.21	7.2	T	1	VHP
NS_143_N	22/11/1996	21.71	1.1	23.86	1.2	T	1	VHP
AP_143	23/11/1996	0.67	1.1	2.81	1.7	T	1	VHP
NS_145_N	27/11/1996	15.46	0.9	18.01	6.9	T	1	VHP
AP_145	27/11/1996	18.83	0.8	21.03	3.8	T	1	VHP
AP_146	30/11/1996	3.83	0.7	6.20	5.5	T	1	VHP
NS_146_S	30/11/1996	6.21	0.8	8.81	8.0	T	1	VHP
AP_147	2/12/1996	12.83	0.6	15.57	9.0	T	1	VHP
NS_148_N	4/12/1996	17.29	0.3	19.56	4.7	T	1	VHP
AP_148	4/12/1996	21.83	0.2	23.88	0.3	T	1	VHP
AP_149	7/12/1996	6.92	0.3	9.52	9.2	T	1	VHP
NS_150_N	9/12/1996	12.63	0.1	15.34	8.8	T	1	VHP
AP_150	9/12/1996	15.92	0.0	18.35	5.6	T	1	VHP
AP_151	12/12/1996	1.00	23.6	2.99	3.4	T	1	VHP
NS_151_S	12/12/1996	1.54	23.7	3.58	3.9	T	1	VHP
NS_153_N	16/12/1996	14.13	23.6	16.76	-6.8	T	1	VHP
AP_153	16/12/1996	19.08	23.4	21.11	-2.3	T	1	VHP
AP_154	19/12/1996	4.00	23.2	6.24	7.0	T	1	VHP
NS_154_S	19/12/1996	4.96	23.3	7.30	8.0	T	1	VHP
AP_155	21/12/1996	13.08	23.3	15.71	-7.6	T	1	VHP
NS_156_N	23/12/1996	17.54	23.0	19.64	-3.4	T	1	VHP
AP_156	23/12/1996	22.17	22.8	0.04	1.2	T	1	VHP
NS_158_N	28/12/1996	11.37	22.8	13.85	-9.0	T	1	VHP
AP_158	28/12/1996	16.17	22.6	18.44	-4.2	T	1	VHP

Table 5. SAMPLE OUTPUT OF PREDICTION PROCEDURE (configuartion 5 only)

Cluster Orbit Predictions

****

Station

EISCAT Tromso : Latitude 69.6 : Longitude 19.2

Configurations

5

Event	DD/MM/YYYY	UT	Cluster MLT	Ground MLT	GB_MLT - IMLT	Prediction status	Config	Priority
AO_003_N	25/12/1995	8.46	10.9	10.92	0.0	T	5	VHP
AO_006_N	1/ 1/1996	11.47	10.5	13.93	3.4	T	5	VHP
AO_008_N	6/ 1/1996	5.51	9.8	7.75	-2.0	T	5	VHP
AO_011_N	13/ 1/1996	8.48	9.4	10.77	1.4	T	5	VHP
AO_014_N	20/ 1/1996	11.53	9.1	13.80	4.7	T	5	VHP
AO_134_N	31/10/1996	12.63	14.7	15.28	0.6	T	5	VHP
AO_136_N	5/11/1996	6.73	14.5	9.34	-5.2	T	5	VHP
AO_139_N	12/11/1996	9.84	14.1	12.42	-1.7	T	5	VHP
AO_142_N	19/11/1996	12.96	13.5	15.71	2.2	T	5	VHP
AO_144_N	24/11/1996	6.97	13.2	9.61	-3.6	T	5	VHP
AO_147_N	1/12/1996	10.07	12.7	12.65	-0.0	T	5	VHP
AO_152_N	13/12/1996	7.32	11.8	9.90	-1.9	T	5	VHP
AO_155_N	20/12/1996	10.32	11.4	12.80	1.4	T	5	VHP

Table 6. SAMPLE OUTPUT OF PREDICTION PROCEDURE (all very high priority configurations)

Cluster Orbit Predictions

****

Station

EISCAT Tromso : Latitude 69.6 : Longitude 19.2

Configurations

1 , 5 , 22 , 27 , 32 , 43 , 43* , 45 , 51 , 56 , 56* , 60 , 66

Event	DD/MM/YYYY	UT	Cluster MLT	Ground MLT	GB_MLT - IMLT	Prediction status	Config	Priority
AO_003_N	25/12/1995	8.46	10.9	10.92	0.0	T	5	VHP
AP_004	28/12/1995	20.16	22.6	22.06	-0.5	T	1	VHP
AO_006_N	1/ 1/1996	11.47	10.5	13.93	3.4	T	5	VHP
AP_007	4/ 1/1996	23.33	22.0	1.10	3.1	T	1	VHP
AO_008_N	6/ 1/1996	5.51	9.8	7.75	-2.0	T	5	VHP
AP_009	9/ 1/1996	17.33	21.8	19.35	-2.4	T	1	VHP
NS_009_S	9/ 1/1996	23.54	21.5	1.28	3.8	T	1	VHP
AO_011_N	13/ 1/1996	8.48	9.4	10.77	1.4	T	5	VHP
AP_012	16/ 1/1996	20.33	21.3	22.13	0.8	T	1	VHP
AO_013_N	18/ 1/1996	2.52	9.0	4.38	-4.6	T	45	VHP
AO_014_N	20/ 1/1996	11.53	9.1	13.80	4.7	T	5	VHP
NS_014_S	21/ 1/1996	21.96	20.7	23.70	3.0	T	1	VHP
AO_016_N	25/ 1/1996	5.38	8.4	7.45	-0.9	T	45	VHP
AO_019_N	1/ 2/1996	8.52	8.1	10.64	2.5	T	45	VHP
AO_021_N	6/ 2/1996	2.46	7.6	4.28	-3.3	T	45	VHP
AO_024_N	13/ 2/1996	5.31	7.1	7.30	0.2	T	45	VHP
MP_025_N	16/ 2/1996	15.96	19.3	17.96	-1.3	T	51	VHP
MP_028_N	23/ 2/1996	10.13	18.7	12.13	-0.6	T	43	VHP
MP_028_S	24/ 2/1996	10.87	18.8	12.89	0.1	T	43*	VHP
AO_029_N	25/ 2/1996	2.22	6.4	4.09	-2.3	T	45	VHP
MP_029_N	25/ 2/1996	17.63	19.1	19.58	0.5	T	51	VHP
MP_031_N	1/ 3/1996	9.46	18.1	11.45	-0.6	T	43	VHP
AO_032_N	3/ 3/1996	5.16	5.9	7.15	1.3	T	45	VHP
MP_032_N	3/ 3/1996	17.54	18.8	19.52	0.7	T	51	VHP
MP_033_S	7/ 3/1996	10.96	18.0	12.99	1.0	T	43*	VHP
MP_034_N	8/ 3/1996	10.12	17.8	12.13	0.3	T	43	VHP
MP_035_N	10/ 3/1996	18.62	18.5	20.66	2.2	T	51	VHP
AO_037_N	15/ 3/1996	2.06	5.2	4.05	-1.1	T	45	VHP
MP_037_N	15/ 3/1996	11.79	17.6	13.84	2.2	T	43	VHP
MP_038_S	19/ 3/1996	9.38	17.3	11.42	0.1	T	43*	VHP
AO_040_N	22/ 3/1996	4.93	4.8	7.00	2.2	T	45	VHP
MP_040_N	22/ 3/1996	13.71	17.6	15.65	-2.0	T	51	VHP

(Table 6, continued)

MP_041_S	26/ 3/1996	12.96	16.3	14.95	4.7	T	43*	VHP
MP_042_N	27/ 3/1996	7.29	16.2	9.37	-0.8	T	43	VHP
MP_043_N	29/ 3/1996	16.04	17.6	17.97	0.4	T	51	VHP
MP_043_S	31/ 3/1996	7.21	16.8	9.31	-1.5	T	43*	VHP
AO_045_N	3/ 4/1996	1.84	4.1	3.98	-0.1	T	45	VHP
MP_045_N	3/ 4/1996	9.62	16.3	11.72	1.4	T	43	VHP
MP_046_N	5/ 4/1996	18.46	17.2	20.71	3.5	T	51	VHP
MP_046_S	7/ 4/1996	10.54	15.7	12.67	3.0	T	43*	VHP
AO_048_N	10/ 4/1996	4.88	3.7	7.04	3.3	T	45	VHP
MP_048_N	10/ 4/1996	12.21	16.5	14.27	3.8	T	43	VHP
MP_048_N	10/ 4/1996	12.21	16.5	14.27	-2.2	T	51	VHP
AO_050_N	14/ 4/1996	22.87	3.6	1.16	-2.4	T	45	VHP
MP_050_N	15/ 4/1996	5.96	14.9	8.12	-0.8	T	43	VHP
MP_051_N	17/ 4/1996	14.88	16.7	16.68	-0.0	T	51	VHP
MP_051_S	19/ 4/1996	7.96	15.2	10.11	0.9	T	43*	VHP
MP_053_N	22/ 4/1996	8.71	15.2	10.88	-4.3	T	22	VHP
MP_053_N	22/ 4/1996	8.71	15.2	10.88	1.7	T	27	VHP
MP_054_N	24/ 4/1996	17.71	16.1	20.00	-2.1	T	32	VHP
MP_055_N	27/ 4/1996	2.62	13.6	4.88	-2.7	T	27	VHP
MP_056_N	29/ 4/1996	11.54	15.5	13.68	-1.8	T	22	VHP
MP_058_N	4/ 5/1996	5.38	13.8	7.60	-0.2	T	27	VHP
MP_059_N	6/ 5/1996	14.38	15.7	16.14	0.4	T	22	VHP
MP_059_N	6/ 5/1996	14.38	15.7	16.14	-5.6	T	32	VHP
MP_061_N	11/ 5/1996	8.29	14.2	10.49	-3.7	T	22	VHP
MP_061_N	11/ 5/1996	8.29	14.2	10.49	2.3	T	27	VHP
MP_062_N	13/ 5/1996	17.29	14.6	19.52	-1.1	T	32	VHP
MP_063_N	16/ 5/1996	2.21	12.5	4.51	-2.0	T	27	VHP
MP_064_N	18/ 5/1996	11.21	14.6	13.37	-1.2	T	22	VHP
MP_066_N	23/ 5/1996	5.29	12.9	7.51	0.6	T	27	VHP
MP_067_N	25/ 5/1996	14.29	14.4	16.00	1.6	T	22	VHP
MP_067_N	25/ 5/1996	14.29	14.4	16.00	-4.4	T	32	VHP
MP_069_N	30/ 5/1996	8.21	13.3	10.39	-2.9	T	22	VHP
MP_070_N	1/ 6/1996	17.21	12.5	19.37	0.9	T	32	VHP
MP_071_N	4/ 6/1996	2.29	11.7	4.56	-1.1	T	27	VHP
MP_072_N	6/ 6/1996	11.29	13.5	13.40	-0.1	T	22	VHP
MP_074_N	11/ 6/1996	5.21	12.0	7.38	1.4	T	27	VHP
MP_075_N	13/ 6/1996	14.29	12.8	15.92	-2.9	T	32	VHP
MP_076_N	15/ 6/1996	23.29	10.4	1.74	-2.7	T	27	VHP
MP_077_N	18/ 6/1996	8.37	12.3	10.49	-1.8	T	22	VHP
MP_078_N	20/ 6/1996	17.37	10.2	19.49	3.3	T	32	VHP
MP_079_N	23/ 6/1996	2.37	10.7	4.58	-0.1	T	27	VHP
MP_080_N	25/ 6/1996	11.37	12.2	13.41	1.2	T	22	VHP
MP_082_N	30/ 6/1996	5.46	11.1	7.56	2.5	T	27	VHP
MP_083_N	2/ 7/1996	14.46	10.6	16.02	-0.6	T	32	VHP
MP_084_N	4/ 7/1996	23.46	9.5	1.84	-1.7	T	27	VHP
MP_085_N	7/ 7/1996	8.54	11.2	10.60	-0.6	T	22	VHP
MP_086_N	9/ 7/1996	17.54	8.4	19.64	5.2	T	32	VHP
MP_087_N	12/ 7/1996	2.54	9.8	4.68	0.9	T	27	VHP
MP_088_N	14/ 7/1996	11.62	10.6	13.59	3.0	T	22	VHP
MP_090_N	19/ 7/1996	5.71	10.1	7.76	-2.3	T	22	VHP
MP_090_N	19/ 7/1996	5.71	10.1	7.76	3.7	T	27	VHP
MP_091_N	21/ 7/1996	14.71	8.2	16.25	2.0	T	56	VHP
MP_091_S	23/ 7/1996	8.54	8.3	10.57	-3.7	T	56*	VHP
AO_092_N	23/ 7/1996	17.50	20.7	19.57	-1.1	T	66	VHP
MP_092_N	23/ 7/1996	23.79	8.6	2.09	-0.5	T	27	VHP
MP_093_N	26/ 7/1996	8.79	10.0	10.83	-5.2	T	56	VHP
MP_093_N	26/ 7/1996	8.79	10.0	10.83	0.8	T	60	VHP
MP_094_S	30/ 7/1996	11.46	8.0	13.45	-0.5	T	56*	VHP
AO_095_N	30/ 7/1996	20.69	20.5	23.03	2.5	T	66	VHP

(Table 6, continued)

MP_095_N	31/ 7/1996	2.96	8.9	5.07	-3.8	T	60	VHP
MP_096_N	2/ 8/1996	11.96	8.6	13.91	-0.7	T	56	VHP
AO_097_N	4/ 8/1996	14.67	19.9	16.26	-3.6	T	66	VHP
MP_097_S	6/ 8/1996	14.21	8.0	15.84	1.8	T	56*	VHP
MP_098_N	7/ 8/1996	6.12	9.0	8.17	-0.8	T	60	VHP
MP_099_S	11/ 8/1996	8.04	7.2	10.08	-3.1	T	56*	VHP
AO_100_N	11/ 8/1996	17.81	19.5	19.98	0.5	T	66	VHP
MP_101_N	14/ 8/1996	9.46	8.4	11.54	-2.9	T	56	VHP
MP_102_S	18/ 8/1996	10.71	7.0	12.80	-0.2	T	56*	VHP
MP_103_N	19/ 8/1996	3.63	8.0	5.77	-2.2	T	60	VHP
MP_104_N	21/ 8/1996	12.71	6.4	14.65	2.2	T	56	VHP
AO_105_N	23/ 8/1996	14.83	18.7	16.56	-2.1	T	66	VHP
MP_105_S	25/ 8/1996	13.29	6.8	15.18	2.4	T	56*	VHP
MP_106_N	26/ 8/1996	7.04	7.8	9.15	-4.6	T	56	VHP
MP_106_N	26/ 8/1996	7.04	7.8	9.15	1.4	T	60	VHP
MP_107_S	30/ 8/1996	6.87	6.2	9.01	-3.2	T	56*	VHP
AO_108_N	30/ 8/1996	17.88	18.3	20.13	1.8	T	66	VHP
MP_108_N	31/ 8/1996	1.38	6.9	3.60	-3.3	T	60	VHP
MP_109_N	2/ 9/1996	10.54	6.4	12.70	0.3	T	56	VHP
MP_110_S	6/ 9/1996	9.54	6.0	11.73	-0.3	T	56*	VHP
MP_111_N	7/ 9/1996	5.13	6.9	7.34	0.4	T	60	VHP
AO_113_N	11/ 9/1996	15.16	17.5	17.13	-0.4	T	66	VHP
MP_113_S	13/ 9/1996	11.63	5.7	13.84	2.1	T	56*	VHP
MP_114_N	14/ 9/1996	9.12	5.9	11.35	-0.6	T	56	VHP
AO_116_N	18/ 9/1996	18.11	17.2	20.46	3.3	T	66	VHP
MP_116_N	19/ 9/1996	4.04	6.0	6.33	0.3	T	60	VHP
AO_118_N	23/ 9/1996	12.22	17.0	14.49	-2.5	T	66	VHP
MP_118_S	25/ 9/1996	6.04	4.9	8.37	-2.5	T	56*	VHP
MP_119_N	26/ 9/1996	9.29	4.9	11.60	0.7	T	56	VHP
AO_121_N	30/ 9/1996	15.28	16.5	17.51	1.0	T	66	VHP
MP_121_N	1/10/1996	5.63	5.1	8.00	2.9	T	60	VHP
MP_121_S	2/10/1996	5.88	4.5	8.26	-2.2	T	56*	VHP
MP_123_N	6/10/1996	4.29	4.6	6.67	2.1	T	60	VHP
AO_124_N	7/10/1996	18.41	16.1	20.81	4.7	T	66	VHP
AO_126_N	12/10/1996	12.35	15.9	14.82	-1.1	T	66	VHP
AO_129_N	19/10/1996	15.50	15.3	17.94	2.6	T	66	VHP
NS_132_N	27/10/1996	19.54	2.9	21.90	5.0	T	1	VHP
AP_132	27/10/1996	21.42	2.8	23.73	3.1	T	1	VHP
AO_134_N	31/10/1996	12.63	14.7	15.28	0.6	T	5	VHP
NS_135_N	3/11/1996	21.46	2.4	23.74	2.7	T	1	VHP
AP_135	4/11/1996	0.50	2.4	2.75	0.3	T	1	VHP
AO_136_N	5/11/1996	6.73	14.5	9.34	-5.2	T	5	VHP
AO_139_N	12/11/1996	9.84	14.1	12.42	-1.7	T	5	VHP
AP_140	15/11/1996	21.67	1.5	23.88	1.6	T	1	VHP
AO_142_N	19/11/1996	12.96	13.5	15.71	2.2	T	5	VHP
NS_143_N	22/11/1996	21.71	1.1	23.86	1.2	T	1	VHP
AP_143	23/11/1996	0.67	1.1	2.81	1.7	T	1	VHP
AO_144_N	24/11/1996	6.97	13.2	9.61	-3.6	T	5	VHP
AP_145	27/11/1996	18.83	0.8	21.03	3.8	T	1	VHP
AO_147_N	1/12/1996	10.07	12.7	12.65	-0.0	T	5	VHP
AP_148	4/12/1996	21.83	0.2	23.88	0.3	T	1	VHP
AP_150	12/12/1996	1.00	23.6	2.99	3.4	T	1	VHP
AO_152_N	13/12/1996	7.32	11.8	9.90	-1.9	T	5	VHP
AP_153	16/12/1996	19.08	23.4	21.11	-2.3	T	1	VHP
AO_155_N	20/12/1996	10.32	11.4	12.80	1.4	T	5	VHP
AP_156	23/12/1996	22.17	22.8	0.04	1.2	T	1	VHP

Legends to figures

Figure 1. Cluster orbits for when the orbit plane is close to the noon-midnight (GSE XZ) plane. The Earth and the Cluster orbit (thick line) are viewed from dusk and the small arrows show the location of a ground observatory. The thin lines show a typical magnetopause location, along with geomagnetic field lines which thread the dayside low-latitude boundary layer (LLBL), the high latitude boundary layer (HLBL or mantle) and the tail neutral sheet. The numbers refer to satellite locations for configurations/conjunctions with the ground observatory which we have identified to be of particular scientific interest (see Table 1). The upper row of four figures are all for orbits with satellite apogee in the midnight sector and the lower row are for apogee in the noon sector. The vertical columns are for the sector in which the ground-based observatory is situated at time when the satellite is at the numbered location (from left to right, the plots in each horizontal row are for the ground-based observatory in the midnight, dawn, noon and dusk sectors). Note that because the ground observatory rotates as the satellite moves along the orbit, the numbered configurations occur in a complex sequence. Configurations where the ground station and Cluster are in opposite hemispheres are denoted with an asterix.

Figure 2. Corresponding plots to figure 1, for when the orbit plane is close to the dawn-dusk (GSE YZ) plane, so that satellite apogee is in the dusk sector (upper row) or the dawn sector (lower row). The Earth and the Cluster orbit (thick line) are viewed from the sun and the thin lines show a typical magnetopause and field lines which pass through the low-latitude boundary layer on the dawn and dusk flanks of the magnetosphere.

Figure 3. An example of the planned Cluster orbit when apogee, AP, is near noon. The Earth and the GSE XZ plane are viewed from dawn. Tick marks on the orbit are one hour apart. The dashed lines show model predictions of the magnetopause and bow shock, for median interplanetary conditions. The magnetospheric field lines are from the Tsyganenko T89 model. The "events" marked are when Cluster is at a certain part of the orbit or crosses a magnetospheric current sheet or L-shell, defined using the models (see text for details).

Figure 4. Simple representation of the proposed planning cycle for coordinated observations. (see section 5 of text for details).

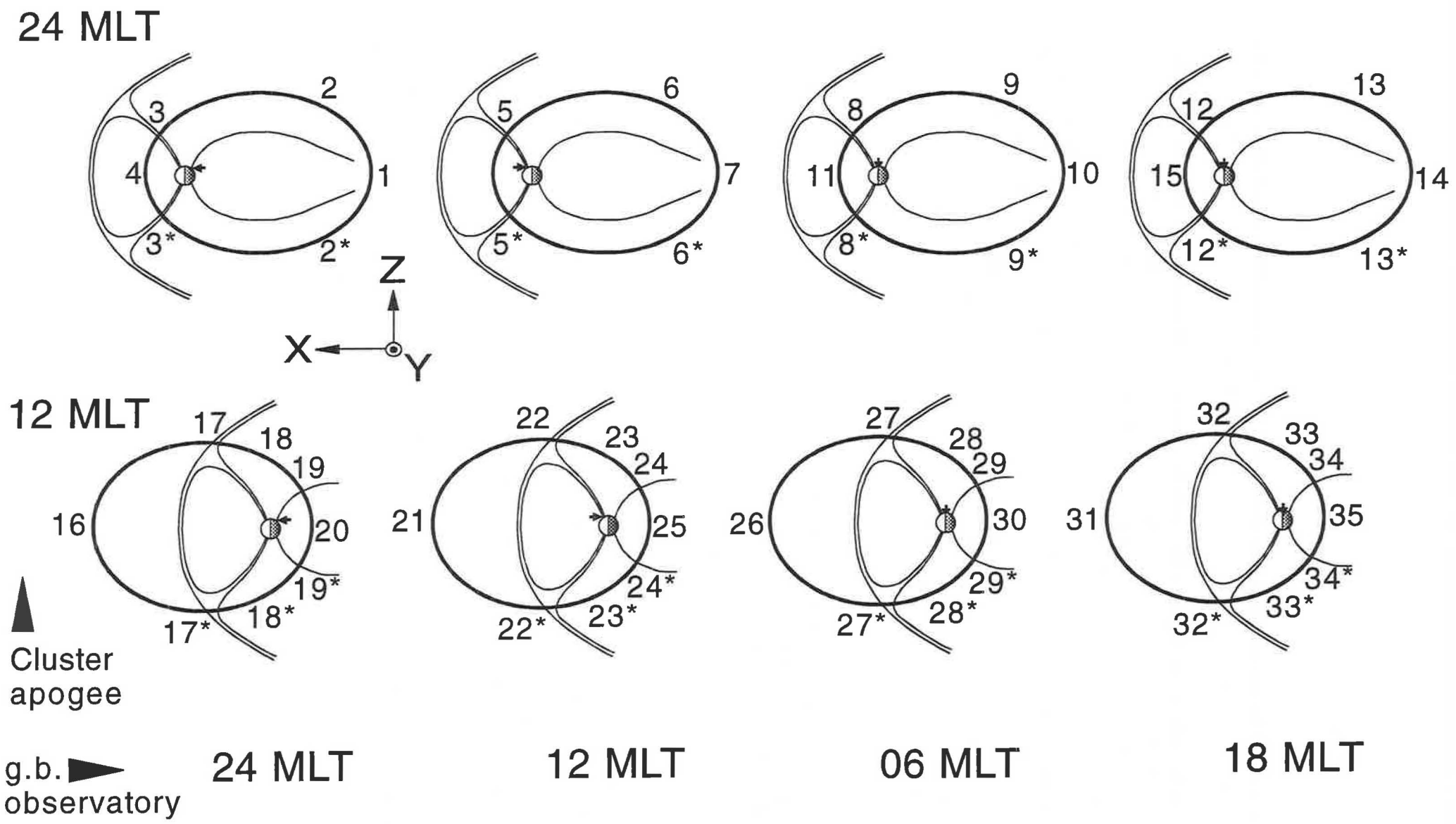
24 MLT
1
2
2*
3
3*
4
5
5*
6
6*
7
8
8*
9
9*
10
11
12
12*
13
13*
14
15
Z
X
Y
12 MLT
16
17
17*
18
18*
19
19*
20
21
22
22*
23
23*
24
24*
25
26
27
27*
28
28*
29
29*
30
31
32
32*
33
33*
34
34*
35
Cluster apogee
g.b. observatory
24 MLT
12 MLT
06 MLT
18 MLT

Figure 1.

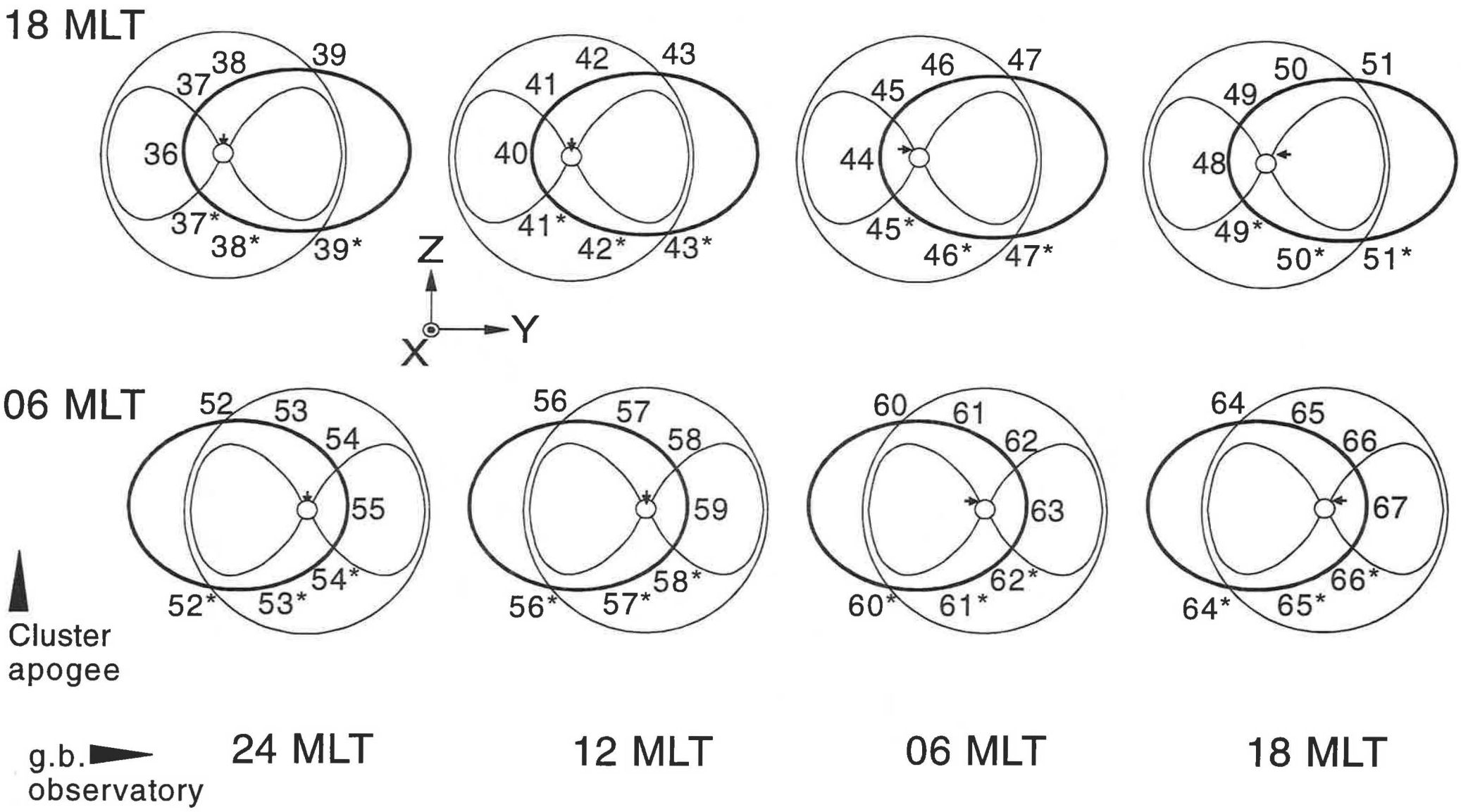
18 MLT
36
37
38
39
37*
38*
39*
40
41
42
43
41*
42*
43*
44
45
46
47
45*
46*
47*
48
49
50
51
49*
50*
51*
Z
Y
X
06 MLT
52
53
54
55
52*
53*
54*
56
57
58
59
56*
57*
58*
60
61
62
63
60*
61*
62*
64
65
66
67
64*
65*
66*
Cluster apogee
g.b. observatory
24 MLT
12 MLT
06 MLT
18 MLT

Figure 2.

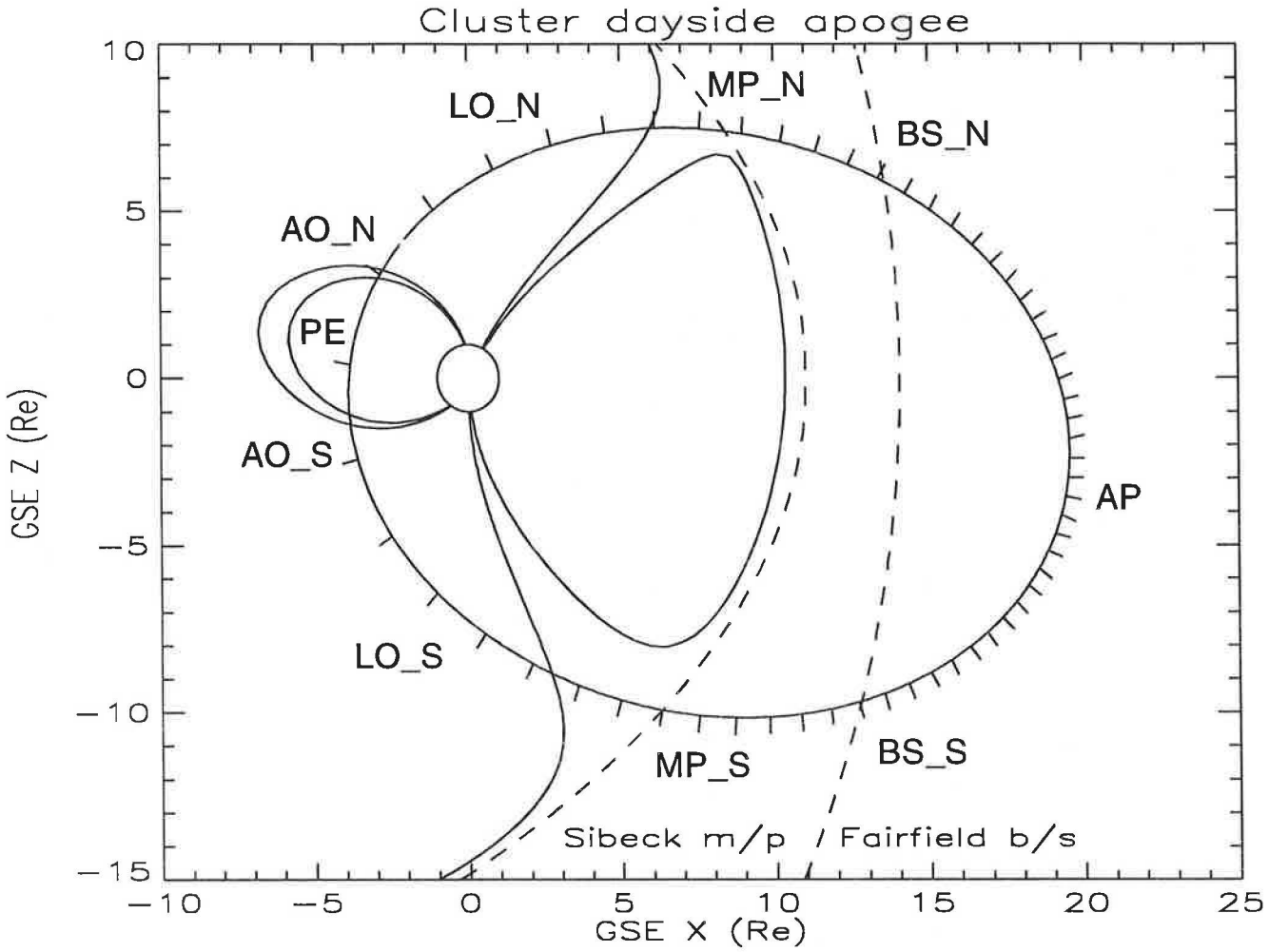
Cluster dayside apogee
LO_N
MP_N
BS_N
AO_N
PE
AO_S
AP
LO_S
MP_S
BS_S
Sibeck m/p / Fairfield b/s
GSE Z (Re)
GSE X (Re)
10
5
0
−5
−10
−15
−10
−5
0
5
10
15
20
25

Figure 3.

Proposed Planning Cycle CLUSTER and Ground-based coordination

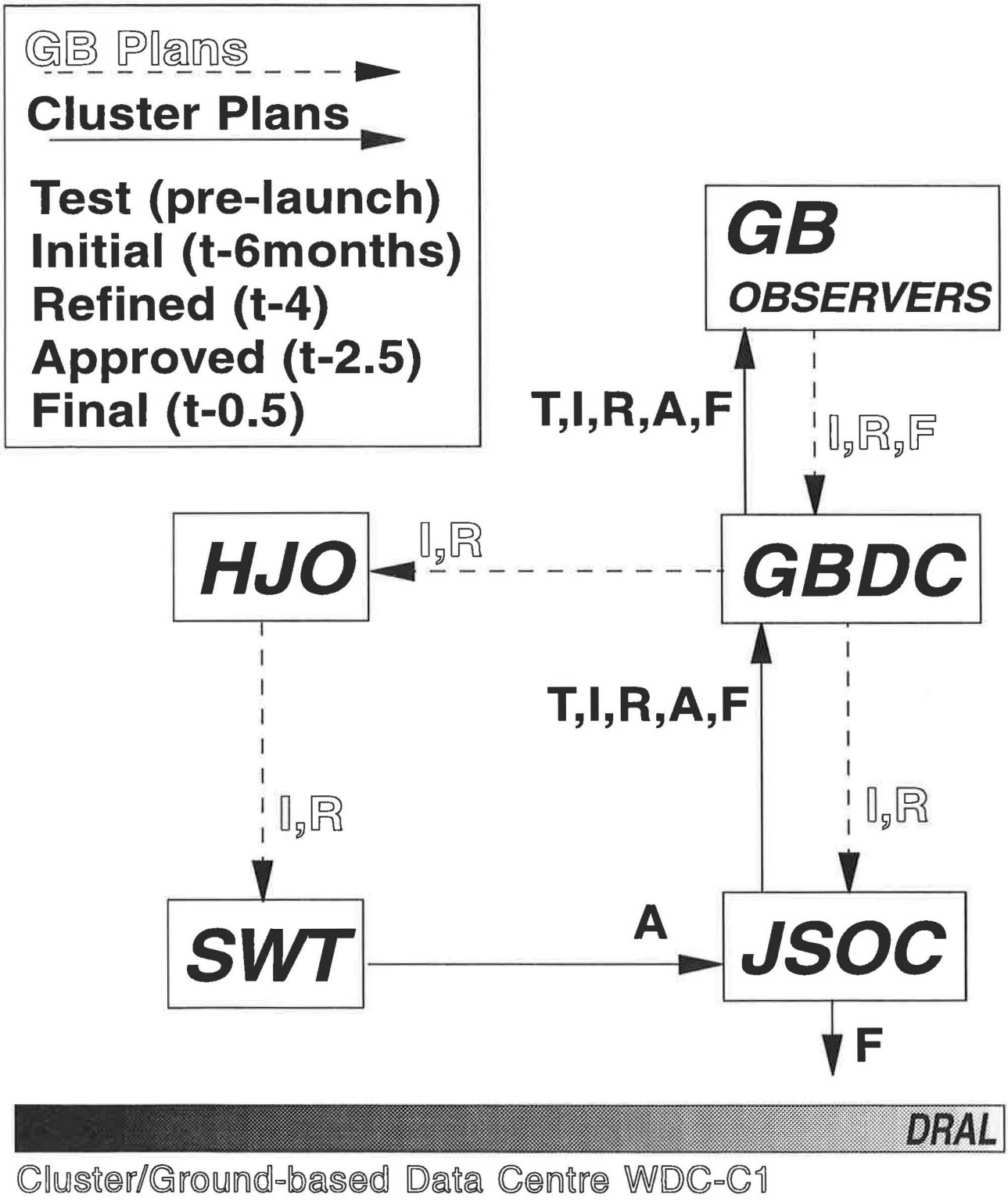

Figure 4.